JOURNAL OF SANDWICH STRUCTURES & MATERIALS

Original Article

Journal of Sandwich Structures and Materials
15(4) 377–411

DOI: 10.1177/1099636213485518
jsm.sagepub.com
SAGE

Free vibration of unidirectional sandwich panels, Part I: Compressible core

Y Frostig[1], CN Phan[2] and GA Kardomateas[2]

Abstract

The free vibration response of a unidirectional sandwich panel with a compressible and incompressible core using the various computational models is presented and compared with closed-form elasticity solutions and finite element results. The mathematical formulations for various models along with the numerical investigation are presented in two parts. In the first part compressible core are considered using the elasticity closed-form solution and various high-order computational models such as the high-order sandwich panel theory (HSAPT) and the extended HSAPT model (EHSAPT). The second part is dedicated to incompressible cores and includes classical models, first-order and high-order shear deformable models, and zig-zag displacement pattern model, ordinary sandwich panel theory. The elasticity-based model serving as the benchmark solution (in first part) assumes isotropic, orthotropic, as well as layered core types. The mathematical formulation utilizes Hamilton's principle to derive the general equations of motion. A closed-form solution of the elasticity model is available only for a simply-supported panel and it is compared with all various models numerically. The numerical investigation includes: eigenfrequencies, displacement modes along the length and through the depth of panel, as well as stress modes through the depth of panel. The results of the various models are compared with the 2D elasticity solution and finite element results of ADINA. In general, the lower mode correlates well for all models while for the higher modes only the EHSAPT and the HSAPT with displacement formulation compared well.

Keywords

Sandwich construction, compressible core, high-order, free vibrations, eigenfrequencies, eigenmodes, computational models

[1]Faculty of Civil and Environmental Engineering, Technion-Israel Institute of Technology, Haifa, Israel
[2]School of Aerospace Engineering, Georgia Institute of Technology, Atlanta, GA, USA

Corresponding author:
Y Frostig, Faculty of Civil and Environmental Engineering, Technion-Israel Institute of Technology, Haifa, 32000, Israel.
Email: cvrfros@techunix.technion.ac.il

Introduction

Vibration of modern sandwich flat panels that are used in various industries such as aerospace, mechanical and civil engineering for structural applications starts to emerge as an important topic especially when dynamic or blast lading is considered. A typical panel is usually made of two face sheets, metallic or composite laminated that are very stiff and a core that is usually made of a low-strength light or heavy (dense) foam, or lightweight, low strength metallic honeycomb, or solid light material such as balsa wood or similar. Notice that a foam core is flexible (low rigidity) in all directions; however, in the vertical direction it is the only component that has some rigidity to resist the vertical normal stresses that may reach large values in the vicinity of localized effects. In the in-plane direction the core contribution to the overall bending rigidity of the panel (core and face sheets) is usually very small as compared to that of the face sheets. Hence, in many practical applications the in-plane rigidity of the core is usually neglected. It means that the entire overall bending moment in a section is being carried by the couple that is formed in the face sheets. The contribution of the face sheets to the bending resistance relative to the overall bending is denoted by the term composite action, which is equal to one when the core in-plane resistance is neglected. The case of a metallic honeycomb core represents a core that is very stiff in the vertical direction but very flexible in the in-plane direction. And the other option of a core made of a light solid material defines a core where its in-plane rigidity may be comparable to that of the bending moments due to couple that is formed in the face sheets and in such cases the composite action factor is smaller than one. In general, the approaches taken to analyze such panels is in tandem with the properties of the core and to mention a few: classical with no shear deformation, first-order shear deformation theory (FOSDT), high-order shear deformation theory (HOSDT) (ESL models) that include shear deformations with various kinematic assumptions and some layered models such as the ordinary sandwich panel theory (OSPT), one that are appropriate for the analysis of panels with a metallic honeycomb core; the high-order (layered wise) approaches (high-order sandwich panel theory, HSAPT), have been used for 'soft' compliant low strength core type that are flexible in the vertical directions and with negligible in-plane rigidity, such as light foam or honeycomb; and the case of a core made of a solid materials that requires an appropriate model, which includes the effects of the in-plane and the vertical rigidity of the core on the response such as the extended high-order sandwich panel theory (EHSAPT). Details on the various models and references are described ahead in the two papers. One of the typical errors involved in the analysis of sandwich panels is the use of models that are appropriate for incompressible core to analyze panels with a soft (compressible) core especially in dynamic problems. In general, the eigenmodes of a panel consist of overall ones as well as through the thickness as a result of displacements in the vertical direction. However, when incompressible core models are used no through thickness modes are detected. Hence, in order to identify the effects of the various core types on the response some well-known computational models are studied and compared. The article has two major

goals: the first is the accurate mathematical description of the incompressible and compressible computational models and the second is to demonstrate what is the accuracy of the compressible core models and to what extent is the use of the incompressible core models in describing the response of *any* type of sandwich panels being correct.

In general, the analysis of sandwich panel follows two main tracks that are in tandem with the core type. The first one assumes that the cores are an anti-plane type, i.e. very stiff in the vertical directions and with negligible in-plane rigidity in the longitudinal direction [1–3], which correlates well with the response of sandwich panel made of a metallic honeycomb core and maybe modeled by the incompressible core approaches such as the FOSDT, HOSDT or OSPT models. The second track is the high-order models that are appropriate for low strength, flexible foam cores and combines the layers of the face sheets and the core into an overall structure through equilibrium and compatibility, see, for example, Frostig et al. [4].

In addition, there is an approach that is based on elasticity that assumes that the sandwich panel consists of 2D elasticity layers, i.e. the face sheets and the core are interconnected through equilibrium and compatibility. An approach based on elasticity formulation assuming linear small deformation kinematic relations has been taken by: Pagano [5] for composite and sandwich panels; Pagano and Hatfield [6] for bidirectional composite panels; Zenkour [7], Kardomateas [8,9] and Kardomateas and Phan [10] for a static and buckling analysis; Srinivas and Rao [11] for dynamic response of simply-supported composite panels; and recently Karczmarzyk [12] for dynamic response of clamped–clamped sandwich panel using a special type of analytical solution. In general, these solutions are quite limited since closed-form solutions exist for only simply-supported panels or panels with specially prescribed BCs. Hence, they may serve as a benchmark rather than as a general computational tool. Here, this solution is used as a benchmark for the free vibration of a simply-supported sandwich panel.

A different approach when compared with the equivalent single layer (ESL) [3] assumes that the sandwich panels are made of layers that are interconnected through equilibrium and compatibility, the core is compliant, compressible with negligible in-plane rigidity, denoted as the high-order sandwich panel theory (HSAPT). This approach has been used for static, dynamic, linear and non-linear applications and to mention a few: beam analysis [4]; buckling and free vibration [13,14]; non-linear behavior [15]; free vibration of curved panels [16]; free vibrations of plates [17]; dynamic response of debonded panels [18,19] and recently, free vibration with thermal effects [20,21].

An improvement of the HSAPT model for panels is required when the cores in-plane rigidity cannot be neglected, such as solid medium to heavy weight foam or wood; or when the response of the panel is of a local type such as wrinkling. In such cases, an enhanced high-order sandwich panel theory [EHSAPT] should be used. It has been recently implemented [22] for application of in-plane loads through core, for wrinkling and global buckling of sandwich panels [23,24] and for dynamic applications [25].

The references previously mentioned consist of a mathematical formulation that presents the equations of motion, including rotational inertia that are derived explicitly through the Hamilton principle and the specific mass and stiffness matrices for a simply-supported case. In general, it follows the steps of the high-order theory (HSAPT) used for unidirectional panels and plates [4,13,14,16]. In the formulation it is assumed that the panels are elastic, linear with small displacements and they consist of a core and two thin plates – two face sheets, with in-plane and flexural rigidity and negligible shear rigidity. In addition, all cores have vertical shear resistance with negligible in-plane resistance. But in the case of incompressible core the vertical rigidity is infinite while in the compressible ones it is finite and usually small. The EHSAPT is the only model that includes the in-plane rigidity of the core. In addition, face–core interfaces fulfill the conditions of full bond with shear and vertical normal stress resistances.

The article consists of two main sections. In the first section the mathematical formulation of the elasticity and the high-order models, HSAPT and EHSAPT, are presented that includes the equations of motion (PDEs) and the appropriate mass and stiffness matrices for the case of a simply-supported panel. In the second section a numerical investigation is presented for a specific configuration that has been used for blast experiment panel with a single- and a multi-layered core. Finally, a summary is presented and conclusions are drawn.

Mathematical formulation

The equations of motion for the various models have been derived or re-derived through the Hamilton principle that uses the variation of the kinetic and internal energy. It reads

$$\delta L = \int_{t_1}^{t_2} (\delta T - \delta U) \mathrm{d}t = 0 \tag{1}$$

where L is the Lagrangian, T is the kinetic energy, U is the internal potential energy, t is the time coordinate between the times t_1 and t_2 and δ denotes the variation operator.

The first variation of the kinetic energy for the sandwich panel reads

$$\begin{aligned} \delta T = \int_{t_1}^{t_2} \Bigg(& \int_{V_t} \rho_t u_{t,t} \delta u_{t,t} + \rho_t w_{t,t} \delta w_{t,t} \, \mathrm{d}v + \int_{V_b} \rho_b u_{b,t} \delta u_{b,t} + \rho_b w_{b,t} \delta w_{b,t} \, \mathrm{d}v \\ & + \int_{V_c} \rho_c u_{c,t} \delta u_{c,t} + \rho_c w_{c,t} \delta w_{c,t} \, \mathrm{d}v \Bigg) \mathrm{d}t \end{aligned} \tag{2}$$

where ρ_j $(j = t, b, c)$ is the mass density of the upper and lower face sheets and the core respectively; $u_{j,t}$ and $w_{j,t} (j = t, b, c)$ are the velocities in the longitudinal and

vertical direction respectively of the various constituents of the sandwich panel; $f_{,t} = \frac{\partial f}{\partial t}$ is the first derivative of the function f with respect to the time coordinate; $V_j (j = t, b, c)$ is the volume of upper and lower face sheets and core, respectively and dv is the volume of a differential segment.

The first variation of the internal potential energy is general and it is formulated to be applicable to all computational models through the special α, β and λ terms. It is defined in terms of stresses and strains and reads

$$\delta U = \int_{V_t} \sigma_{xxt}\delta\varepsilon_{xxt} + \alpha_f \tau_{xzt}\delta\gamma_{xzt}\,dv + \int_{V_b} \sigma_{xxb}\delta\varepsilon_{xxb} + \alpha_f \tau_{xzb}\delta\gamma_{xzb}\,dv + \int_{V_c} \lambda_c \sigma_{xxc}\delta\varepsilon_{xxc} + \alpha_c \tau_{xzc}\delta\gamma_{xzc} + \beta_c \sigma_{zzc}\delta\varepsilon_{zzc}\,dv$$

where

$$\varepsilon_{xxj}(x, z_j, t) = \frac{\partial}{\partial x} u_j(x, z_j, t), \quad \varepsilon_{zzj}(x, z_j, t) = \frac{\partial}{\partial z_j} w_j(x, z_j, t)$$
$$\gamma_{xzj}(x, z_j, t) = \frac{\partial}{\partial z_j} u_j(x, z_j, t) + \frac{\partial}{\partial x} w_j(x, z_j, t) \qquad (j = t, b, c) \qquad (3)$$

And σ_{xxj} and ε_{xxj} $(i = x$ and $j = t, b)$ are the longitudinal normal stresses and strains in the upper and the lower face sheet, respectively; τ_{xzj} and $\gamma_{xzj} (j = t, b)$ are the vertical shear stress and angle respectively at the various face sheets; τ_{xzc} and γ_{xzc} are the vertical shear stresses and shear strains in the core on the longitudinal and transverse faces of the core, respectively; σ_{zzc} and ε_{zzc} are the vertical normal stresses and strains in the vertical direction of the core and u_j and $w_j (j = t, b, c)$ are the displacements in the longitudinal and vertical directions respectively of the various constituents of the panel. Geometry and sign convention for stresses and displacements are shown in Figures 1 to 4.

The energy terms for the various computational model are controlled through the α, β and λ terms as follows: HSAPT – $\alpha_f = \lambda_c = 0$, $\alpha_c = \beta_c = 1$, EHSAPT – $\alpha_f = 0$, $\lambda_c = \alpha_c = \beta_c = 1$ and ELAS (Elasticity), $\alpha_f = \alpha_c = \beta_c = \lambda_c = 1$.

The formulation ahead outlines the 2D elasticity solution, proceeds with the high-order and extended high-order models.

2D elasticity model

The equations of motion in terms of stresses and displacements as a result of the Hamilton principle and the kinetic and potential energies (equations (1) to (3)), for any layer of the sandwich panel, face sheets (t, b) or core (c), read

$$\left(\frac{\partial}{\partial x}\sigma_{xxj}(x, z_j, t) + \frac{\partial}{\partial z_j}\tau_{xzj}(x, z_j, t) - \rho_j \frac{\partial^2}{\partial t^2} u_j(x, z, t)\right) b_w = 0$$

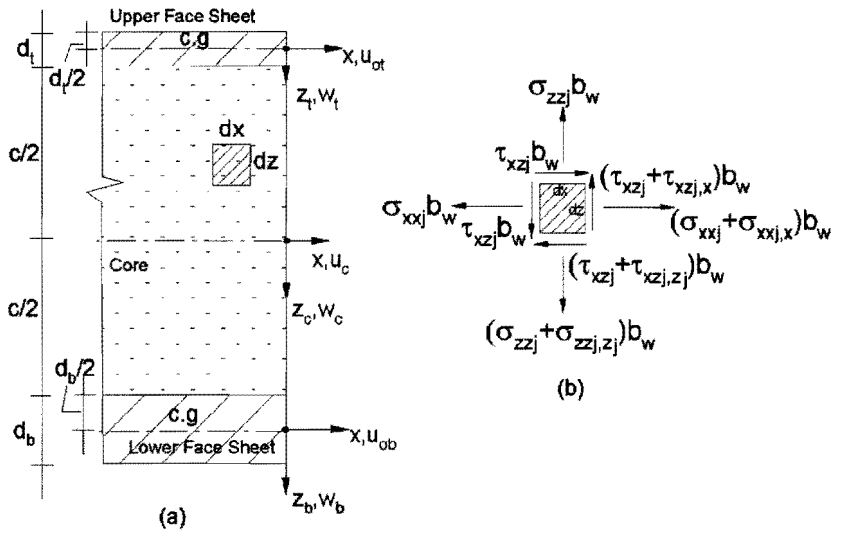

Figure 1. Coordinate system and stresses for the elasticity model: (a) coordinate system and (b) stresses within a layer.

$$\left(\frac{\partial}{\partial x}\tau_{xzj}(x,z_j,t)+\frac{\partial}{\partial z_j}\sigma_{zz}(x,z_j,t)-\rho_j\frac{\partial^2}{\partial t^2}w_j(x,z_j,t)\right)b_w=0 \tag{4}$$

where $\sigma_{kkj}(k=x,z,j=t,c,b)$ are the normal stresses in the longitudinal and vertical direction respectively at the various layers; τ_{xzj} is the shear stresses in the j layer; u_j and w_j are the displacements in the longitudinal and vertical directions, respectively; x and z_j are the coordinates in the longitudinal and the vertical (local coordinate) directions, respectively; ρ_j is the mass density of the various layers and b_w is the width of the panel. Notice that the stresses and the displacements are general functions of the space and time coordinates. Sign convention, coordinates, and stresses on a differential element are provided in Figure 1.

The stresses following Hook law in terms of the displacements assuming an orthotropic material in the j layer read

$$\sigma_{xxj}=\frac{E_{xj}\left(\frac{\partial}{\partial x}u_j(x,z_j,t)+\nu_{zxj}\frac{\partial}{\partial z_j}w_j(x,z_j,t)\right)}{1-\nu_{xzj}\nu_{zxj}},\quad \sigma_{zzj}=\frac{E_{zj}\left(\frac{\partial}{\partial z_j}w_j(x,z_j,t)+\nu_{xzj}\frac{\partial}{\partial x}u_j(x,z_j,t)\right)}{1-\nu_{xzj}\nu_{zxj}}$$
$$\tau_{xzj}=G_{xzj}\left(\frac{\partial}{\partial z_j}u_j(x,z_j,t)+\frac{\partial}{\partial x}w_j(x,z_j,t)\right) \tag{5}$$

where $E_{kj}(k=x,z)$ and G_{xzj} are the moduli of elasticity in the longitudinal and vertical directions respectively and the shear modulus of the j layer; ν_{xzj} and ν_{zxj} are the Poisson's ratio in longitudinal and vertical directions, respectively.

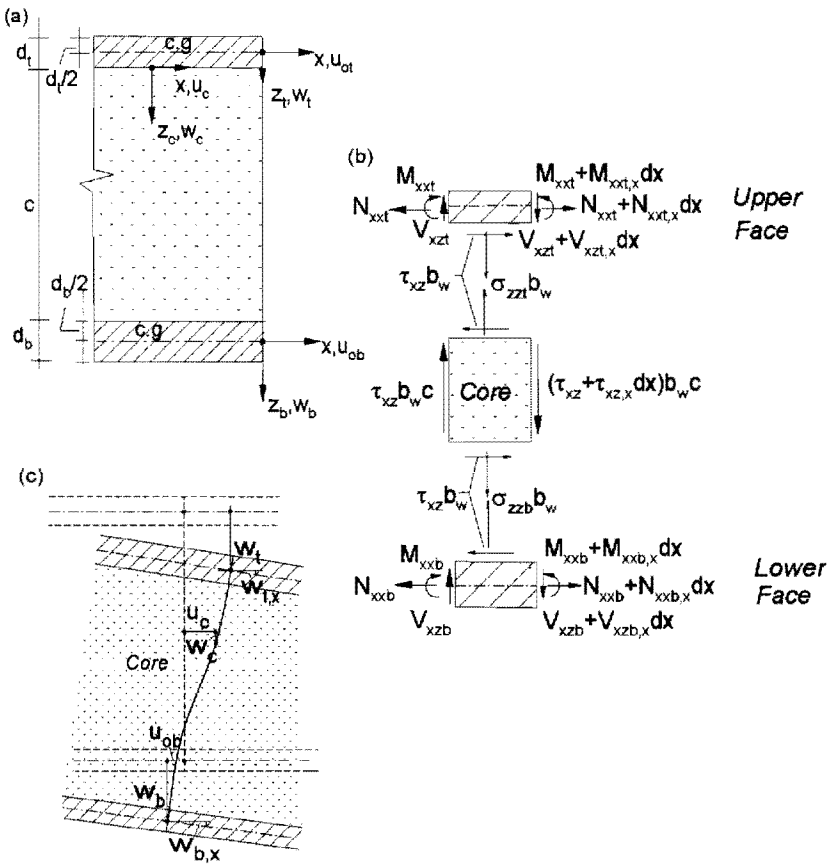

Figure 2. Coordinate system, stress resultants and displacement pattern for the HSAPT with mixed formulation model: (a) coordinate system; (b) stress resultants and (c) displacement pattern through depth of panel.
HSAPT: high-order sandwich panel theory.

A simply-supported panel is considered here since it is only case where the elasticity model has an accurate closed-form solution. The formulation ahead takes a similar approach to that of Pagano [5] and Srinivas and Rao [11] with modification as a result of the existence of a low strength compliant core. Thus the displacements read

$$u_j(x, z_j, t) = \sum_{m=1}^{N} u_{mj}(z_j)\cos(\alpha_m x)e^{I\omega_m t}, \quad w_j(x, z_j, t) = \sum_{m=1}^{N} w_{mj}(z_j)\sin(\alpha_m x)e^{I\omega_m t} \quad (6)$$

where $u_{mj}(z_j)$ and $w_{mj}(z_j)$ are the displacements in the longitudinal and vertical directions through the depth of layer j that correspond to the half wave number m,

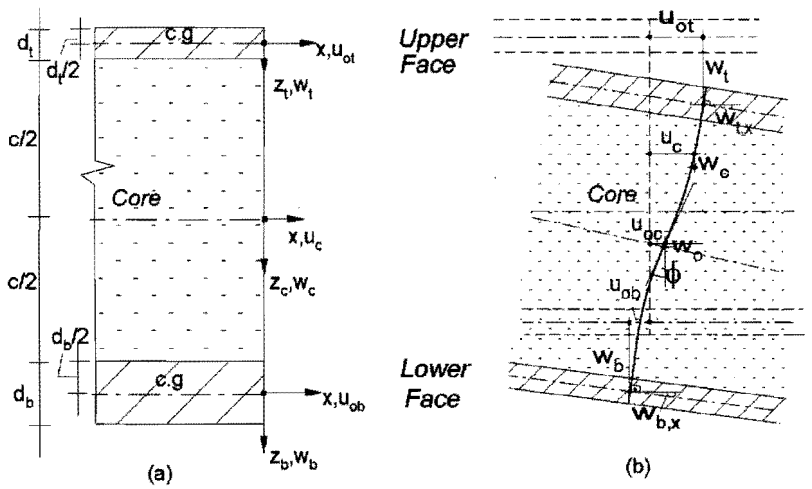

Figure 3. Coordinate system and displacement pattern for the HSAPT with displacement formulations: (a) coordinate system and (b) displacement pattern through depth of panel.
HSAPT: high-order sandwich panel theory.

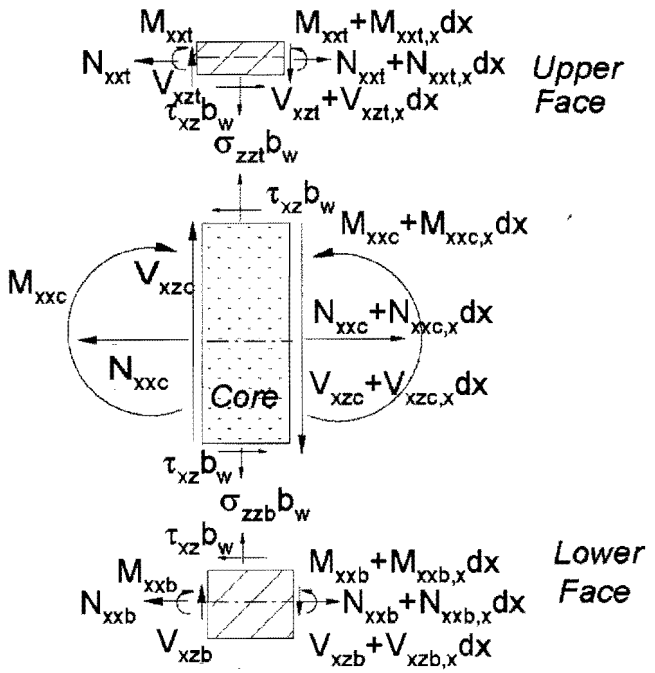

Figure 4. Stress resultants and displacement pattern for the EHSAPT model.
EHSAPT: extended high-order sandwich panel theory.

respectively; $\alpha_m = m\pi/L$ with L being the length of the panel and N the number of half waves; $I=\sqrt{-1}$, ω_m is the eigenfrequency of the m wave number and t is the time coordinate.

The formulation ahead uses a single term solution for brevity due to the uncoupling between the equations of each terms of the series solution. Hence, the equations of motion are defined through substitution of the single term displacements (equations (6)), into the stresses (equations (5)), and then into the equilibrium equations (equations (4)). Hence, they read

$$\begin{aligned}
&\left(\left(\frac{\mathrm{d}}{\mathrm{d}z_j}w_{mj}(z_j)\right)\alpha_m + \frac{\mathrm{d}^2}{\mathrm{d}z_j^2}u_{mj}(z_j)\right)G_{xzj} + \left(\rho_j\omega_m^2 + \frac{E_{xj}\alpha_m^2}{-1+\nu_{xzj}\nu_{zxj}}\right)u_{mj}(z_j) \\
&\quad - \frac{\nu_{zxj}E_{xj}\left(\frac{\mathrm{d}}{\mathrm{d}z_j}w_{mj}(z_j)\right)\alpha_m}{-1+\nu_{xzj}\nu_{zxj}} = 0 \\
&\frac{\alpha_m\left(\frac{\mathrm{d}}{\mathrm{d}z_j}u_{mj}(z_j)\right)\left(G_{xzj}(1-\nu_{xzj}\nu_{zxj})+E_{zj}\nu_{xzj}\right)}{-1+\nu_{xzj}\nu_{zxj}} - \alpha_m^2 w_{mj}(z_j)G_{xzj} + \rho_{mj}\omega_m^2 w_{mj}(z_j) \\
&\quad - \frac{E_{zj}\frac{\mathrm{d}^2}{\mathrm{d}z_j^2}w_{mj}(z_j)}{-1+\nu_{xzj}\nu_{zxj}} = 0
\end{aligned} \tag{7}$$

In the case of an isotropic layer: $E_{xj} = E_{zj} = E_j$, $\nu_{xzj} = \nu_{zxj} = \mu_j$, a closed-form solution exists and it reads

$$\begin{aligned}
u_j(z_j) &= C_1\mathrm{e}^{\sqrt{\beta_1}z_j} + C_2\mathrm{e}^{-\sqrt{\beta_1}z_j} + C_3\mathrm{e}^{\sqrt{\beta_2}z_j} + \mathrm{e}^{-\sqrt{\beta_2}z_j}C_4 \\
w_j(z_j) &= \frac{\left(-\mathrm{e}^{-\sqrt{\beta_2}z_j}C_4 + C_3\mathrm{e}^{\sqrt{\beta_2}z_j}\right)\alpha_m}{\sqrt{\beta_2}} + \frac{\left(-C_2\mathrm{e}^{-\sqrt{\beta_1}z_j} + C_1\mathrm{e}^{\sqrt{\beta_1}z_j}\right)\sqrt{\beta_1}}{\alpha_m}
\end{aligned} \tag{8}$$

where $\beta_1 = \alpha_m^2 + \dfrac{\left(-1+\mu_j^2\right)\rho_j\omega_m^2}{E_{zj}}$, $\beta_2 = \alpha_m^2 - 2\dfrac{\rho_j(1+\mu_j)\omega_m^2}{E_{zj}}$

And C_k ($k=1,2,3,4$) are the constants of integration to be determined by equilibrium and compatibility through depth of panel or the stress-free surfaces conditions. In addition, the stresses for this case read

$$\sigma_{xx}(x,z_j,t) = -\frac{E_j\sin(\alpha_m x)\mathrm{e}^{I\omega t}\left(\begin{array}{l}\left(C_2\mathrm{e}^{-\sqrt{\beta_1}z_j} + C_1\mathrm{e}^{\sqrt{\beta_1}z_j}\right)\left(-\alpha_m^2+\mu_j\beta_1\right) \\ +\left(\mathrm{e}^{-\sqrt{\beta_2}z_j}C_4 + C_3\mathrm{e}^{\sqrt{\beta_2}z_j}\right)\alpha_m^2(-1+\mu_j)\end{array}\right)}{\alpha_m\left(-1+\mu_j^2\right)}$$

$$\sigma_{zz}(x,z_j,t)=\frac{E_j\sin(\alpha_m x)e^{I\omega t}\left(\begin{array}{l}\left(e^{-\sqrt{\beta_2}z_j}C_4+C_3e^{\sqrt{\beta_2}z_j}\right)\alpha_m^2(-1+\mu_j)\\ \quad+\left(C_2e^{-\sqrt{\beta_1}z_j}+C_1e^{\sqrt{\beta_1}z_j}\right)(-\beta_1+\alpha_m^2\mu_j)\end{array}\right)}{\alpha_m\left(-1+\mu_j^2\right)}$$

$$\tau_{xz}(x,z_j,t)=2\frac{e^{I\omega t}\cos(\alpha_m x)G_{xzj}\left(\begin{array}{l}\left(-1/2e^{-\sqrt{\beta_2}z_j}C_4+1/2C_3e^{\sqrt{\beta_2}z_j}\right)(\alpha_m^2+\beta_2)\\ \quad+\left(-C_2e^{-\sqrt{\beta_1}z_j}+C_1e^{\sqrt{\beta_1}z_j}\right)\sqrt{\beta_2}\sqrt{\beta_1}\end{array}\right)}{\sqrt{\beta_2}} \tag{9}$$

In the case of a honeycomb or a low-strength compliant core, which has shear and vertical normal stresses rigidity and neglected in-plane rigidity, the mechanical properties equal or approximated respectively as follows: $E_{xj}=0$, $E_{zj}=E_j$, $\nu_{xzj}=\nu_{zxj}=\mu_j$. And in this case the closed-form solution read

$$u_j(z_j)=\frac{-1/4\sqrt{\beta_4}\sqrt{E_j^{-1}}\sqrt{2}}{\alpha_m\rho_j\omega_m^2(1+\mu_j)^2}\times\left(\begin{array}{l}\left(C_4e^{1/2z_j\sqrt{\beta_{4a}}}-C_3e^{-1/2z_j\sqrt{\beta_{4a}}}\right)\left(\sqrt{\beta_2}+\left(\begin{array}{l}-2\mu_j\omega_m^2\\ -\mu_j^2\omega_m^2-\omega_m^2\end{array}\right)\rho_j+\alpha_m^2E_j\mu_j\right)\\ \quad+\beta_5\left(C_1e^{-1/2z_j\sqrt{\beta_{3a}}}-e^{1/2z_j\sqrt{\beta_{3a}}}C_2\right)\sqrt{\dfrac{\beta_3}{\beta_4}}\end{array}\right)$$

$$w_j(z_j)=C_1e^{-1/2z_j\sqrt{\beta_{3a}}}+e^{1/2z_j\sqrt{\beta_{3a}}}C_2+C_3e^{-1/2z_j\sqrt{\beta_{4a}}}+C_4e^{1/2z_j\sqrt{\beta_{4a}}}$$

where

$$\beta_1=2E_j\alpha_m^2\rho_j(\mu_j-2)(1+\mu_j)^2\omega_m^2,\quad \beta_2=\rho_j^2(1+\mu_j)^4\omega_m^4-\beta_1+\alpha_m^4E_j^2\mu_j^2$$

$$\beta_3=-\sqrt{\beta_2}+\left(-2\mu_j-3+\mu_j^2\right)\rho_j\omega_m^2-\alpha_m^2E_j\mu_j,$$

$$\beta_4=\sqrt{\beta_2}+\left(-2\mu_j-3+\mu_j^2\right)\rho_j\omega_m^2-\alpha_m^2E_j\mu_j,$$

$$\beta_5=\sqrt{\beta_2}+\left(1+2\mu_j+\mu_j^2\right)\omega_m^2\rho_j-\alpha_m^2E_j\mu_j$$

$$\beta_{3a}=-2\alpha_m^2\mu+\frac{(-4\mu-6+2\mu^2)roc\omega_m^2-2\sqrt{\beta_2}}{E_j}$$

$$\beta_{4a}=-2\alpha_m^2\mu_j+\frac{\left(-4\mu_j-6+2\mu_j^2\right)\rho_j\omega_m^2+2\sqrt{\beta_2}}{E_j} \tag{10}$$

And the stresses read

$$\sigma_{xxj}(x,z_j,t)=0,$$

$$\sigma_{zzj}(x,z_j,t)=-1/2\,e^{i\omega_m t}\sin(\alpha_m x)\begin{pmatrix}\sqrt{\beta_{3a}}\left(C_1 e^{-1/2 z_j\sqrt{\beta_{3a}}}-C_2 e^{1/2 z_j\sqrt{\beta_{3a}}}\right)\\ +\sqrt{\beta_{4a}}\left(C_3 e^{-1/2 z_j\sqrt{\beta_{4a}}}-C_4 e^{1/2 z_j\sqrt{\beta_{4a}}}\right)\end{pmatrix}E_j$$

$$\tau_{xzj}(x,z_j,t)=\frac{1/8\,G_{xj}e^{i\omega_m t}\cos(\alpha_m x)}{\alpha_m\rho_j\omega_m^2(1+\mu_j)^2}\times\begin{pmatrix}\left(\sqrt{\beta_4}\sqrt{E_j^{-1}}\sqrt{2}\beta_5\sqrt{\beta_{3a}}\sqrt{\frac{\beta_3}{\beta_4}}+8\alpha_m^2\rho_j\omega_m^2(1+\mu_j)^2\right)\\ \left(C_1 e^{-1/2 z_j\sqrt{\beta_{3a}}}+e^{1/2 z_j\sqrt{\beta_{3a}}}C_2\right)\\ +\begin{pmatrix}\sqrt{2}\sqrt{\beta_4}\sqrt{\beta_{4a}}\left(-\sqrt{\beta_2}\left(1+2\mu_j+\mu_j^2\right)\omega_m^2\rho_j-\alpha_m^2 E_j\mu_j\right)\\ \times\sqrt{E_j^{-1}}+8\alpha_m^2\rho_j\omega_m^2(1+\mu_j)^2\end{pmatrix}\\ \left(C_3 e^{-1/2 z_j\sqrt{\beta_{4a}}}+C_4 e^{1/2 z_j\sqrt{\beta_{4a}}}\right)\end{pmatrix} \tag{11}$$

The full response of the sandwich panel is a combination of two face sheets and a core, which has properties that are different by order of magnitude, and are interconnected through continuity conditions and free stress surfaces. Hence, in order to determine the constants of integration, C_k, for each layer face sheets and core the following conditions must be fulfilled

$$\begin{aligned}
&-\sigma_{zzt}(x,z_t=-1/2d_t,t)=0,\quad -\tau_{xzt}(x,z_t=-1/2d_t,t)=0\\
&u_t(x,z_t=1/2d_t,t)-u_c(x,z_c=-1/2c,t)=0\\
&w_t(x,z_t=1/2d_t,t)-w_c(x,z_c=-1/2c,t)=0\\
&-\sigma_{zzt}(x,z_t=1/2d_t,t)+\sigma_{zzc}(x,z_c=-1/2c,t)=0\\
&-\tau_{xzt}(x,z_t=1/2d_t)+\tau_{xzc}(x,z_c=-1/2c)=0\\
&u_c(x,z_t=1/2c,t)-u_b(x,z_c=-1/2d_b,t)=0\\
&w_c(x,z_c=1/2c,t)-w_b(x,z_b=-1/2d_b,t)=0\\
&-\sigma_{zzc}(x,z_c=1/2c,t)+\sigma_{zzb}(x,z_b=-1/2d_b,t)=0\\
&-\tau_{xzc}(x,z_c=1/2c,t)+\tau_{xzb}(x,z_b=-1/2d_b,t)=0\\
&\sigma_{zzt}(x,z_b=1/2d_b,t)=0,\quad \tau_{xzb}(x,z_b=1/2d_b,t)=0
\end{aligned} \tag{12}$$

Notice that the first two and the last two conditions refer to stress-free surface requirement while the other eight refer to the interfaces between the face sheets and the core and consist of continuity requirements in displacements and equilibrium in

vertical and longitudinal directions. In addition notice that the full set of equations consists of equations with extremely large differences in magnitude – there are equations in the order of displacements and there are equations in the order of stresses. Hence, a scaling procedure must be used in order to get a reliable numerical scheme.

The same solution can be used for the case of a sandwich panel with a few layers or face sheets that consist of a few layers or a sandwich panel with a few face sheets and in between cores, denoted as multi-layered sandwich panel. The conditions that are required to be fulfilled are stress-free at the outer fibers of the panel and continuity in displacement and equilibrium at interfaces between the layers. Notice the large difference measured by order of magnitudes between the stress and the displacements condition requires a scaling procedure in order to achieve reliable and accurate numerical results.

High-order sandwich panel theory model

Two variants of the HSAPT models are considered. The first one, denoted as HSAPT (mixed) uses the unknowns of the ordinary HSAPT model that includes the displacements of the face sheets, u_{oj} and w_j $(j=t,b)$ along with the shear stresses in the core and the velocities through the depth of the core are assumed to be linear [14]. The second model, denoted by HSAPT (displacement), assumes that the distribution of the displacements and the velocities in the core are polynomial, cubic for the longitudinal displacements and quadratic for vertical one, which corresponds to the static displacement patterns of the HSAPT model [4]. Here, the unknowns consist of the displacements of the face sheets and the coefficients of these polynomials and not the shear stress in the core. For more details in the case of vibration of a 2D sandwich plate see Frostig and Thomsen [17].

The equations of motion are derived through the Hamilton principle (equations (1)) and the variations of the kinetic and potential energy (equations (2) and (3)) along with the following parameters $\alpha_f=0$, $\lambda_c=\alpha_c=\beta_c=1$. The first model is described in detail.

Mixed formulation. Only the equations of motion and mass and stiffness matrixes that correspond to the particulars of a simply-supported panel are presented for completeness and brevity. For more details see Frostig and Baruch [14].

The equations of motion derived from the Hamilton principle (equation (1)), yields only four equations with five unknowns, u_{oj} and w_j $(j=t,b)$ and τ. The fifth equation is the compatibility at the lower face–core interface in the longitudinal direction [14] and they read

$$\left(\frac{1}{3}u_{ot,tt}+\frac{1}{12}w_{b,xtt}d_b-\frac{1}{6}w_{t,xtt}d_t+\frac{1}{6}u_{ob,tt}\right)M_c+u_{ot,tt}M_t-EA_tu_{ot,xx}-\tau b_w c=0$$

$$\left(\left(-\frac{1}{2}c-\frac{1}{2}d_t\right)\tau_x+\frac{(-w_b+w_t)E_c}{c}\right)b_w-w_{t,xxtt}I_{mt}+M_tw_{t,tt}+EI_tw_{t,xxxx}$$
$$+\left(\frac{1}{3}w_{t,tt}+\frac{1}{6}w_{b,tt}+\frac{1}{24}w_{b,xxtt}d_bd_t+\frac{1}{6}u_{ot,xtt}d_t-\frac{1}{12}w_{t,xxtt}d_t^2+\frac{1}{12}u_{o,bxtt}d_t\right)M_c=0$$
$$\left(\frac{1}{3}u_{ob,tt}+\frac{1}{6}u_{ot,tt}-\frac{1}{12}w_{t,xtt}d_t+\frac{1}{6}w_{b,xtt}d_b\right)M_c+\tau b_w-EA_bu_{ob,xx}+M_bu_{ob,tt}=0$$
$$\left(\left(-\frac{1}{2}c-\frac{1}{2}d_b\right)\tau_x+\frac{(w_b-w_t)E_c}{c}\right)b_w-w_{b,xxtt}I_{mb}+EI_bw_{b,xxxx}+M_bw_{b,tt}$$
$$+\left(\frac{1}{6}w_t+\frac{1}{24}w_{t,xxtt}d_td_b-\frac{1}{6}u_{o,bxtt}d_b-\frac{1}{12}w_{b,xxtt}d_b^2-\frac{1}{12}u_{ot,xtt}d_b+\frac{1}{3}w_{b,tt}\right)M_c=0$$
$$\frac{c\tau}{G_c}+\left(-\frac{1}{2}c-\frac{1}{2}d_b\right)w_{b,x}+u_{ot}+\left(-\frac{1}{2}c-\frac{1}{2}d_t\right)w_{t,x}-\frac{1}{12}\frac{c^3\tau_{xx}}{E_c}-u_{ob}=0 \qquad (13)$$

where $f_{k,s}=\frac{\partial}{\partial S}f_k$ or $f_{k,s}=\frac{\partial^2}{\partial S^2}f(x,t)=x$ or t and f is one of the dependent variables; $M_j=\rho_jb_wd_j$ and $I_{mj}=\rho_jb_wd_j^3/12$ $(j=t,b)$ are the mass and the moment of inertia, respectively, of the section of the face sheets and $M_c=\rho_cb_wc$ is the mass of the core section. Notice that only the first four equations have inertia terms while the fifth one is a compatibility equation.

Also here, in the case of a simply-supported panel a solution based on a trigonometric series yield a closed-form solution and it reads

$$u_{oj}=\sum_{m=1}^{N}C_{uoj,m}\cos(\alpha_mx)e^{i\omega_mt},\quad w_j=\sum_{m=1}^{N}C_{wj,m}\sin(\alpha_mx)e^{i\omega_mt}\quad(j=t,b)$$
$$\tau=\sum_{m=1}^{N}C_{\tau,m}\cos(\alpha_mx)e^{i\omega_mt} \qquad (14)$$

where $C_{uoj,m}$ and $C_{wj,m}$ are respectively the constants of the in-plane and vertical displacements of the face sheets and $C_{\tau,m}$ is the constant of the shear stress in the core that correspond to the m half wave number. They are to be determined through the solution of the eigenvalue problem (equation (7)). Thus, the mass and stiffness matrices along with the **C** vector of unknowns read

$$M_m=\begin{bmatrix}\left\{\begin{matrix}(\frac{1}{3}+\frac{1}{12}\alpha_m^2d_t^2)M_c\\+\alpha_m^2I_{mt}+M_t\end{matrix}\right\} & (\frac{1}{6}-\frac{1}{24}\alpha_m^2d_bd_t)M_c & -\frac{1}{6}M_c\alpha_md_t & -\frac{1}{12}M_c\alpha_md_t & 0\\ (\frac{1}{6}+\frac{1}{24}\alpha_m^2d_bd_t)M_c & (\frac{1}{3}+\frac{1}{12}\alpha_m^2d_b^2)M_c+M_b+\alpha_m^2I_{mb} & \frac{1}{2}M_c\alpha_md_b & \frac{1}{6}M_c\alpha_md_b & 0\\ -\frac{1}{6}M_c\alpha_md_t & \frac{1}{12}M_c\alpha_md_b & \frac{1}{3}M_c+M_t & \frac{1}{6}M_c & 0\\ -\frac{1}{12}M_c\alpha_md_t & -\frac{1}{6}M_c\alpha_md_b & \frac{1}{6}M_c & M_b+\frac{1}{3}M_c & 0\\ 0 & 0 & 0 & 0 & 0\end{bmatrix}$$

$$K_m = \begin{vmatrix} EI_t\alpha_m^4 + \frac{b_w E_c}{c} & -\frac{b_w E_c}{c} & 0 & 0 & \frac{1}{2}\alpha_m b_w(d_t + c) \\ -\frac{b_w E_c}{c} & \frac{b_w E_c}{c} + EI_b\alpha_m^4 & 0 & 0 & \frac{1}{2}\alpha_m b_w(d_b + c) \\ 0 & 0 & EA_t\alpha_m^2 & 0 & -b_w \\ 0 & 0 & 0 & EA_b\alpha_m^2 & b_w \\ \frac{1}{2}\alpha_m b_w(d_t + c) & \frac{1}{2}\alpha_m b_w(d_b + c) & -b_w & b_w & -\frac{b_w c}{G_c} - \frac{1}{12}\frac{b_w c^3 \alpha_m^2}{E_c} \end{vmatrix}$$

$$C_m = \left[C_{uot,m}, C_{wt,m}, C_{uob,m}, C_{wb,m}, C_{\tau,m}\right]^T \tag{15}$$

Notice that for each wave number yields only four eigenvalues since the fifth row in the mass matrix is null.

Displacement formulation. In this formulation, the displacement patterns through the depth of the core of the unidirectional panel is assumed to consist of a quadratic and cubic polynomial form for the vertical and longitudinal displacements, respectively [4] (Figure 3(b)). Here, the coefficients of the polynomial are the unknowns rather than the shear stress in the core (see previous sub-section where the displacement pattern in the face sheets follows the Euler–Bernoulli assumption with negligible shear deformation). Hence, the assumed displacements in the face sheets and the core read

$$\begin{aligned} u_j(x, z_j, t) &= u_{oj}(x, t) - z_j(w_{j,x})(x, t) \quad (j = t, b) \\ u_c(x, z_c, t) &= u_{oc}(x, t) + \phi(x, t)z_c + u_2(x, t)z_c^2 + u_3(x, t)z_c^3 \\ w_c(x, z_c, t) &= w_o(x, t) + w_1(x, t)z_c + w_2(x, t)z_c^2 \end{aligned} \tag{16}$$

where u_{oc}, w_o and ϕ are the longitudinal and vertical displacements and the rotation at the centroid of the core, respectively. Coordinate system and displacement patterns are shown in Figure 3. The requirement of full bond at the face core interfaces between the face sheets and the core requires the following compatibility conditions

$$\begin{aligned} &u_c(x, z_c = -1/2c, t) = u_{ot}(x, t) - 1/2d_t(w_{t,x})(x, t), \quad w_c(x, z_c = -1/2c, t) = w_t(x, t) \\ &u_c(x, 1/2z_c = 1/2c, t) = u_{ob}(x, t) + 1/2d_b(w_{b,x})(x, t), \quad w_c(x, z_c = 1/2c, t) = w_b(x, t) \end{aligned} \tag{17}$$

Hence, four out of the seven unknowns in the core displacements can be determined. Hence, after some algebraic manipulation they read

$$\begin{aligned} u_c(x, z_c, t) = &\left(-4\frac{u_{ot}}{c^3} + 2\frac{w_{t,x}d_t}{c^3} - 4\frac{u_1}{c^2} + 4\frac{u_{ob}}{c^3} + 2\frac{w_{b,x}d_b}{c^3}\right)z_c^3 \\ &+ \left(2\frac{u_{ot}}{c^2} - \frac{w_{t,x}d_t}{c^2} + 2\frac{u_{ob}}{c^2} + \frac{w_{b,x}d_b}{c^2} - 4\frac{u_{oc}(x, t)}{c^2}\right)z_c^2 + \phi_c + u_{oc} \end{aligned}$$

$$w_c(x, z_c, t) = w_o + \frac{(-w_t + w_b)z_c}{c} + 2\frac{(w_t - 2w_o + w_b)z_c^2}{c^2} \tag{18}$$

The number of unknowns in this model is only seven, two for each face sheets and three in the core. In addition, the stresses in the core consist of shear and vertical normal stresses while the in-plane stresses are negligible and following Hook law they read:

$$\sigma_{zzc}(x, z_c, t) = E_{zc}\varepsilon_{zzc}(x, z_c, t), \quad \tau(x, z_c, t) = G_{xzc}\gamma(x, z_c, t) \tag{19}$$

And in terms of the unknowns they equal

$$\tau_c(x, z_c, t) = \left(2\frac{z_c^2\left((3d_b + c)w_{b,x} + (c + 3d_t)w_{t,x} - 6u_{ot} - 2w_{o,x}c - 6\phi c + 6u_{ob}\right)}{c^3} + \frac{\left((2d_b + c)w_{b,x} + (-2d_t - c)w_{t,x} + 4u_{ot} - 8u_{oc} + 4u_{ob}\right)z_c}{c^2} + \phi + w_{o,x}\right)G_{xzc}$$

$$\sigma_{zzc}(x, z_c, t) = \left(4\frac{(w_t - 2w_o + w_b)z_c}{c^2} + \frac{w_b - w_t}{c}\right)E_{zc}, \quad \sigma_{xxc}(x, z_c, t) = 0 \tag{20}$$

For details, see similar results for a 2D sandwich plate in Frostig and Thomsen [17].

The equations of motion are derived using the displacements in equations (18) along with the strains defined in lower part of equations (3) and the variation of the kinetic and potential energies (equations (2)), and upper part of equations (3) and the Hamilton principle (equation (1)). The equations are very long and appear in Appendix 1 for brevity.

In the case of a simply-supported panel a closed-form solution in the form of trigonometric series exist that yields an eigenvalue problem and it reads

$$\begin{aligned}
u_{ot} &= \sum_{m=1}^{N} C_{uot,m}\cos(\alpha_m x)e^{I\omega_m t}, \quad w_t = \sum_{m=1}^{N} C_{wt,m}\sin(\alpha_m x)e^{I\omega_m t},\\
u_{ob} &= \sum_{m=1}^{N} C_{uob,m}\cos(\alpha_m x)e^{I\omega_m t}, \quad w_b = \sum_{m=1}^{N} C_{wb,m}\sin(\alpha_m x)e^{I\omega_m t},\\
\phi &= \sum_{m=1}^{N} C_{\phi,m}\cos(\alpha_m x)e^{I\omega_m t}, \quad u_{oc} = \sum_{m=1}^{N} C_{uo,m}\cos(\alpha_m x)e^{I\omega_m t},\\
w_o &= \sum_{m=1}^{N} C_{wo,m}\sin(\alpha_m x)e^{I\omega_m t}
\end{aligned} \tag{21}$$

where $C_{j,m}$ ($j=uot$, wt, uob, wb, uoc, ϕ and wo) are constants to be determined through the eigenvalue solution of the equations of motion given in matrix form as follows

$$(\mathbf{M}_m - \lambda_m \mathrm{K}_m)C_m = \mathbf{0} \tag{22}$$

where $\lambda_m = \omega_m^2$; $C_m^T = [C_{uot,m}, C_{wt,m}, C_{\mathrm{uob,m}}, C_{wb,m}, C_{uoc,m}, C_{\phi,m}, C_{wo,m}]$, and $\mathbf{0}$ is a zero vector of length seven and $\mathbf{M}_m$ and $\mathbf{K}_m$ are the mass and the stiffness matrices, respectively, and ω_m is the radial eigenfrequency of wave number m.

The mass and stiffness matrices are determined through substitution of the solution series into the equations of motion and collecting them with respect to the trigonometric and harmonic functions and the constants of the solution. The matrices are lengthy and are not presented for brevity. Here, the matrices are 7×7 as compared with the previous case of 4×4 after condensation. Hence, this theory predicts seven eigenvalues for each half wave number.

Extended HSAPT model

The EHSAPT model takes into account the in-plane rigidity of the panel and it yields results that almost coincide with some available 2D static elasticity solutions [23,24]. The formulations here includes only the basic equations for brevity and for details see Phan [25]. The extended model assumes that the displacement patterns for the face sheets are those of Euler–Bernoulli while those of the core are polynomial (equations (16)). Hence, after use of compatibility conditions at the face–core interfaces the core displacements change into equations (17) and its stresses appear in equations (18). Here, the in-plane rigidity of the core is considered and therefore the stress fields in the core include normal stresses in longitudinal and vertical directions as well as shear stresses. For the isotropic case they read

$$\sigma_{xxc}(x,z_c) = \left(\begin{array}{l} \left(-4\dfrac{\phi_x}{c^2} + \dfrac{-4u_{ot,x} + 4u_{ob,x} + 2w_{b,xx}d_b + 2d_t w_{t,xx}}{c^3}\right) z_c^3 \\ + \dfrac{(2u_{ot,x} + 2u_{ob,x}(x,t) + w_{b,xx}d_b - 4u_{oc,x} - w_{t,xx}d_t) z_c^2}{c^2} \\ + \left(\dfrac{(-8w_o + 4w_b + 4w_t)\mu_c}{c^2} + \phi_x\right) z_c + \dfrac{(w_b - w_t)\mu_c}{c} + u_{oc,x} \end{array} \right) E_{zc}(1-\mu_c^2)^{-1}$$

$$\sigma_{zzc}(x,z_c) = \left(\begin{array}{l} \left(-4\dfrac{\phi_x}{c^2} + \dfrac{-4u_{ot,x} + 4u_{ob,x} + 2d_b w_{b,xx} + 2d_t w_{t,xx}}{c^3}\right) \mu_c z_c^3 \\ + \dfrac{(2u_{ot,x} + 2u_{ob,x} + d_b w_{b,xx} - 4u_{oc,x} - d_t w_{t,xx})\mu_c z_c^2}{c^2} \\ + \left(\mu_c \phi_x + \dfrac{-8w_o + 4w_b + 4w_t}{c^2}\right) z_c + \mu_c u_{oc,x} + \dfrac{w_b - w_t}{c} \end{array} \right) E_{zc}(1-\mu_c^2)^{-1}$$

$$\tau_c(x,z_c) = \left(\begin{array}{l} \left(\dfrac{2w_{t,x} - 4w_{o,x} + 2w_{b,x} - 12\phi}{c^2} + \dfrac{-12u_{ot} + 6d_b w_{b,x} + 6d_t w_{t,x} + 12u_{ob}}{c^3} \right) z_c^2 \\ + \left(\dfrac{-w_{t,x} + w_{b,x}}{c} + \dfrac{4u_{ot} - 2\left(\frac{\partial}{\partial x}(x,t)\right) d_t w_{t,x} + 2d_b w_{b,x} - 8u_{oc} + 4u_{ob}}{c^2} \right) z_c \\ + \phi + w_{o,x} \end{array} \right) G_{xzc} \tag{23}$$

In addition, as a result of the in-plane rigidity of the core, there are stress resultants such as axial forces, bending moments, and even higher order bending moments (Figure 4).

The equations of motion that appear in Appendix 2 have been derived through substitution of the strains in the potential energy with the following factors: $\alpha_f = 0$, $\lambda_c = \alpha_c = \beta_c = 1$, see equations (3) and the kinetic energy, equation (2) into the Hamilton's principle. For the case of a simply-supported panel the solution series is the one that appears in equation (21).

The mass and the stiffness matrices are derived through substitution of the trigonometric solution into the equations of motion (see Appendix 2), removing the trigonometric functions, collecting the terms with respect to the constants C_j that appear in equations (21). The explicit description of these matrices appears in Phan's thesis [25]. Also here the size of the matrices is 7 × 7 similar to that of the HSAPT with the displacement formulation. However, the terms in the matrices are totally different due to the contribution of the in-plane rigidity of the core.

Numerical study

The numerical study investigates the free vibration of compressible simply-supported sandwich panel. Single- and multi-layered core based on a specific setup used in the experimental blast investigation of Gardner et al. [26], with some modifications, is adopted here. The results include the eigenfrequencies for the first and the second half wave numbers. The eigenmodes are presented for the case with a low density core.

Single-layered core

The first case investigates the free vibration of a sandwich panel where a single uniform core is based on setup of Gardner et al. [26]. It uses a sandwich panel that consists of face sheets made of E-Glass vinyl-ester laminated composite with a quasi-isotropic layup $[0/45/90/-45]_s$, with a density of 1800 kg/m^3 and an equivalent modulus of elasticity of 13,600 MPa. The foam core, A300, is Corecell^{TM} A-series styrene acrylonitrile (SAN) foams with density of 58.5 kg/m^3, an elasticity modulus of 32 MPa, a Poisson's ratio of 0.25 and a shear modulus of 12.8 MPa.

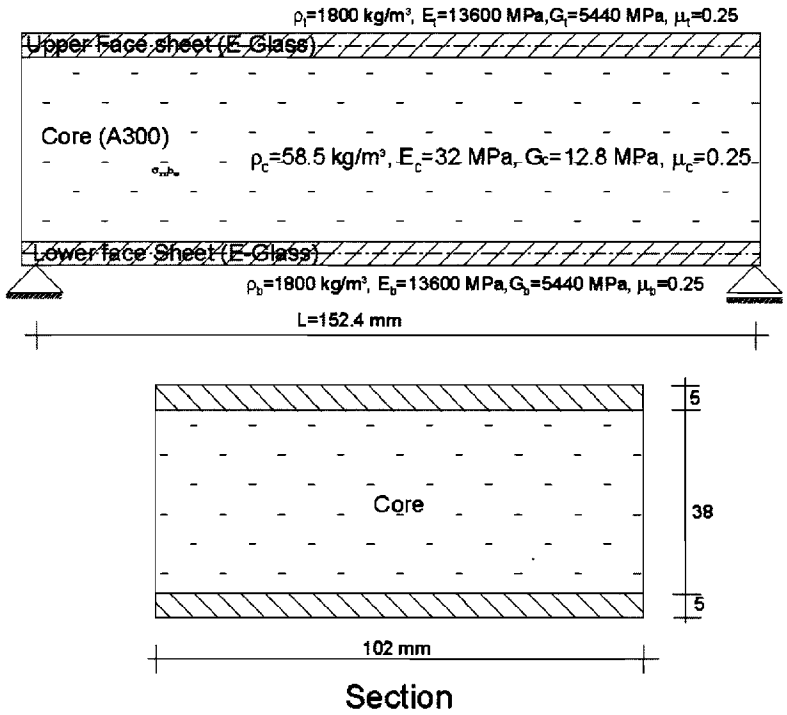

Figure 5. Layout of a sandwich panel with a single-layered core and a typical section.

For geometry see Figure 5. The second case consists of a sandwich panel with a core that is made of a number of layers and a polyurea layer (Figure 7), yielding an unsymmetrical construction layout. For more details on the setup see Gardner et al. [26].

The eigenfrequencies are presented in a non-dimensional form with respect to an eigenfrequency of a unidirectional panel with an identical flexural rigidity only. The results in Table 1 include the eigenfrequencies of: a light core of A300 ($\rho = 58.5\,\mathrm{kg/m^3}$, $E_c = 32\,\mathrm{MPa}$, $G_c = 12.8\,\mathrm{MPa}$, $\mu_c = 0.25$), (for the first two half-wave numbers) a heavy core of A800 ($\rho = 150\,\mathrm{kg/m^3}$, $E_c = 117\,\mathrm{MPa}$, $G_c = 46.8\,\mathrm{MPa}$, $\mu_c = 0.25$) (for the first half-wave only). The eigenmodes of the first wave number along the panel and through the depth of the panel appear in Figures 6 and 7, respectively.

The results in Table 1 consist of four modes for the HSAPT model with the mixed formulation, and seven modes for the HSAPT model with the displacement formulation and the EHSAPT. In addition, there is a column with the results of a finite element (FE) model of ADINA for comparison and the number of values in each computational model corresponds to the number of unknowns in the formulation. However, due to the non-linear eigenvalue problem in the elasticity model the number of modes for each half-wave number is infinite. Here only the first

Table 1. Non-dimensional eigenfrequencies of modes for first and the second half-waves for light (L, A300) and heavy (H, A800) core.

		Computational model				
Mode no.	Wave no.	HSAPT (Mixed)	HSAPT (Displ)	EHSAPT	Elasticity	FE-ADINA
1	$N=1$(L)	0.163	0.164	0.164	0.164	0.163
	$N=1$(H)	0.285	0.286	0.286	0.286	
	$N=2$(L)	0.099	0.100	0.100	0.099	
2	$N=1$(L)	0.569	0.567	0.575	0.574	0.574
	$N=1$(H)	1.136	1.138	1.127	1.134	
	$N=2$(L)	0.157	0.156	0.156	0.156	
3	$N=1$(L)	2.251	1.576	1.704	1.691	1.704
	$N=1$(H)	2.252	1.824	1.982	1.980	
	$N=2$(L)	1.126	0.411	0.529	0.332	
4	$N=1$(L)	2.365	2.331	2.335	2.332	2.391
	$N=1$(H)	2.558	2.514	2.530	2.526	
	$N=2$(L)	1.172	0.688	0.694	0.519	
5	$N=1$(L)		2.463	2.471	2.455	2.499
	$N=1$(H)		2.949	2.986	2.942	
	$N=2$(L)		0.845	0.918	0.682	
6	$N=1$(L)		2.737	2.808	2.781	2.780
	$N=1$(H)		3.757	3.852	3.799	
	$N=2$(L)		1.189	1.190	0.895	
7	$N=1$(L)		3.462	3.536	3.422	3.420
	$N=1$(H)		4.590	4.686	4.521	
	$N=2$(L)		1.206	1.208	1.141	

HSAPT: high-order sandwich panel theory; EHSAPT: extended high-order sandwich panel theory.

seven eigenfrequencies of this model are presented. The two HSAPT models and the EHSAPT model yielded accurate eigenfrequencies for the first two wave number and the first two modes. The HSAPT with the mixed formulation yields quite accurate modes for the first two wave numbers. The discrepancies are larger for the second wave number. The results of the HSAPT model with the displacement formulation and the EHSAPT models compared very well with the elasticity ones. The results are very accurate for the first two modes while the larger discrepancies occur at the third mode for the HSAPT results. In the higher modes the results of the HSAPT are in closer proximity as compared with the EHSAPT. In the case of the second half waves the discrepancies of the third mode and

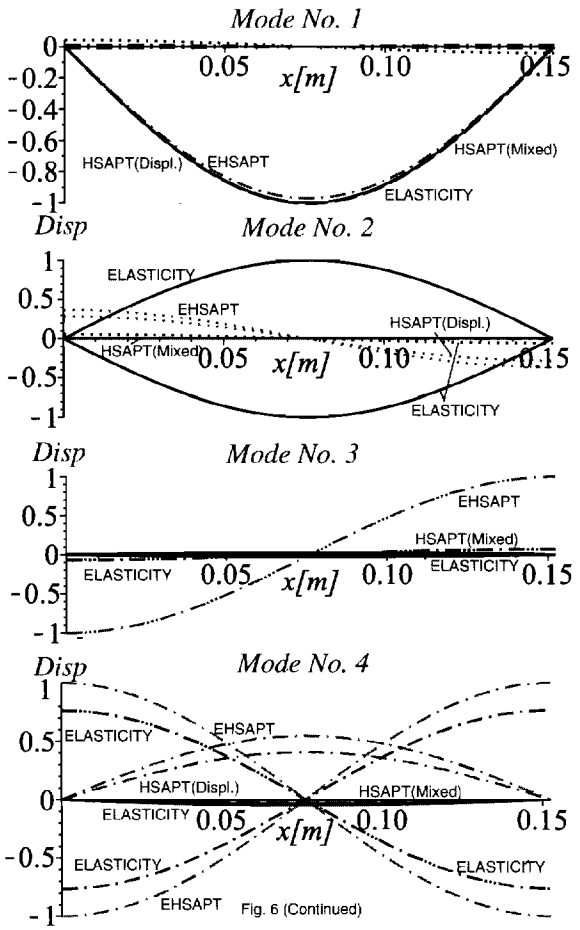

Figure 6. Seven eigenmodes of displacements of the first half-wave number along panel for various computational models and the elasticity solution.
HSAPT: high-order sandwich panel theory; EHSAPT: extended high-order sandwich panel theory.

above is about 5–6% as compared with 1–2% for those of the first half wave number. In addition, the comparison between the light and the heavy core results reveals similar trends for all computational models. The difference between the orthotropic ($E_{xxc}=0$) and the isotropic panels with the elasticity model is minor especially at the lower modes. The FE results compare well with the elasticity eigenfrequencies for the lower modes and the discrepancy becomes larger as the mode number increases.

The eigenmodes along the panel are presented in Figure 6, and through the depth of the panel in Figure 7. They have been determined through normalization with respect to the largest value in the eigenvector of the results while in the elasticity model they have been normalized with respect to the largest displacement

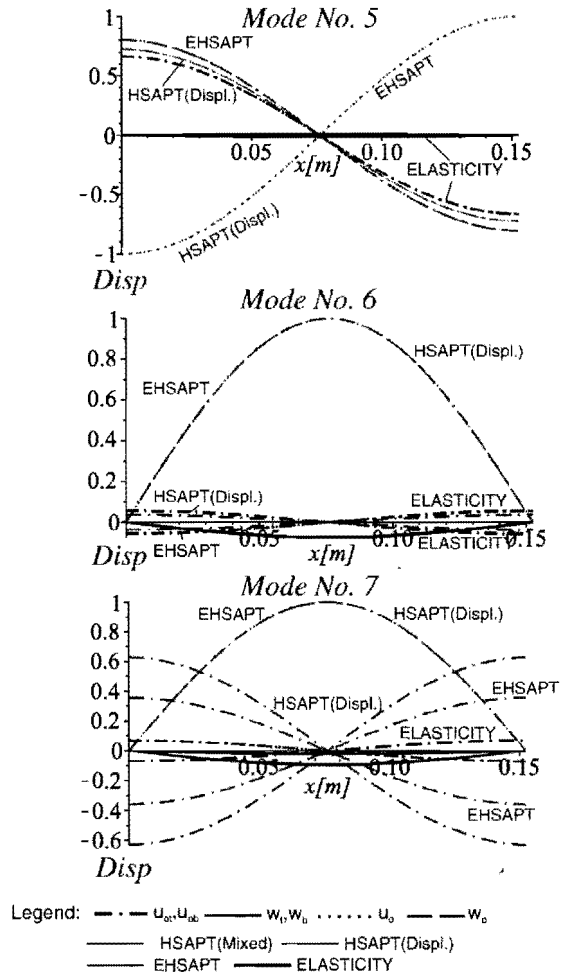

Figure 6. Continued.

through the depth of panel. Notice that the largest value, in the elasticity solution does not necessarily occur at the location of the unknowns of the other computational models. In addition, the modes of the various models have been also normalized with respect to the sign of the corresponding mode of the elasticity model.

The results in Figure 6 describe the in-plane and longitudinal displacements of the upper and the lower face sheets only in the case of the HSAPT (mixed) and in addition, the in-plane and vertical displacements and the rotation at the centroid of the core for the HSAPT (displacement) and EHSAPT models and the elasticity solution includes all the above mentioned normalized unknowns. The first mode corresponds to a pure bending mode where the two face sheets move in tandem and

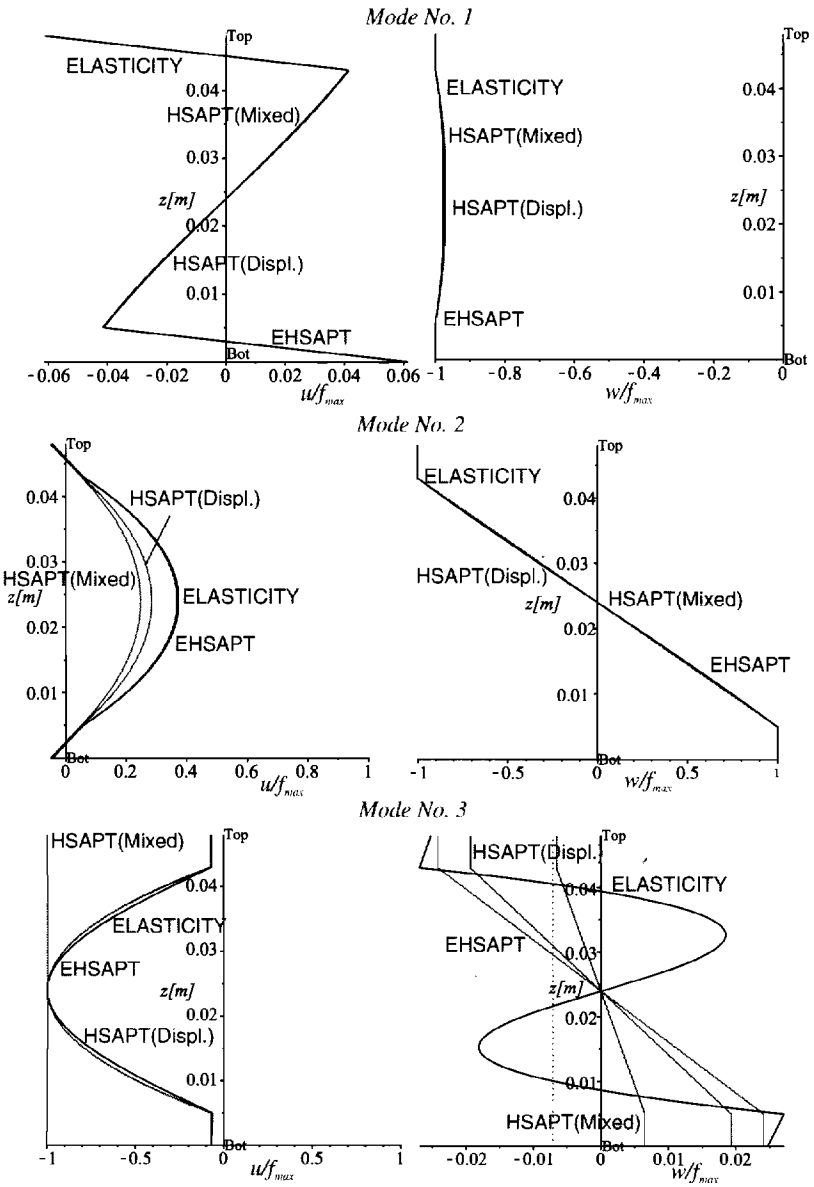

Figure 7. Seven eigenmodes of stresses of the first half-wave number through depth of panel for various computational models and the elasticity solution.
HSAPT: high-order sandwich panel theory; EHSAPT: extended high-order sandwich panel theory.

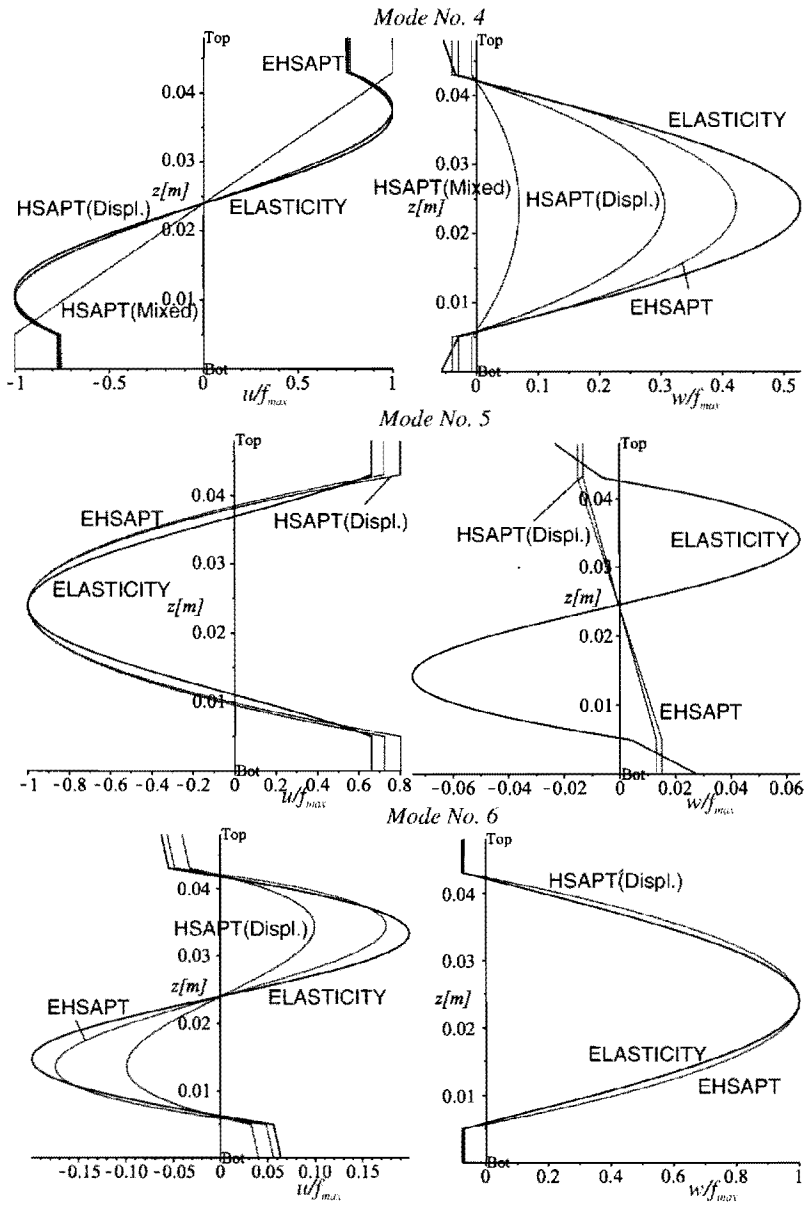

Figure 7. Continued.

is identical for all models. The second mode is a pumping type where the two face sheet move in opposite directions. Here the HSAPT models and the EHSAPT correlate well. The third mode is a longitudinal movement of the face sheets that correlates well with all models although the corresponding eigenfrequencies are

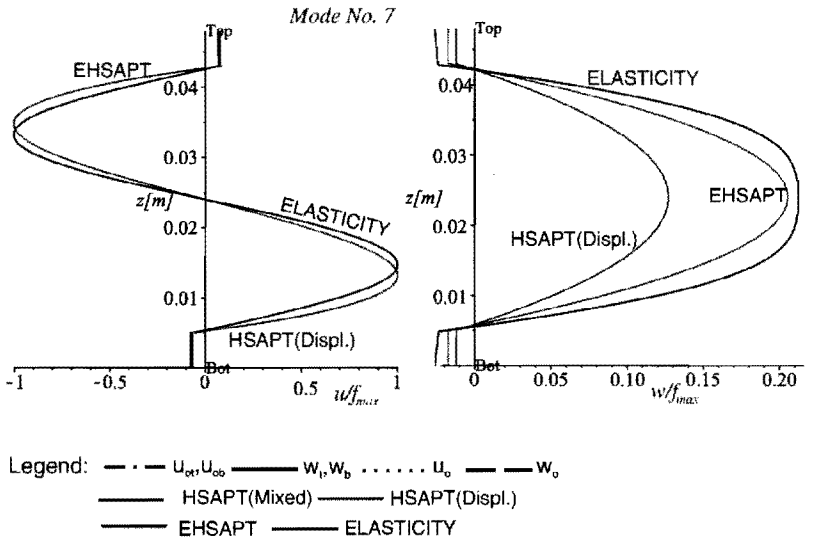

Figure 7. Continued.

quite different. The fourth mode consists of opposite longitudinal displacements of the face sheets with small vertical displacements and it correlate well with HSAPT and EHSAPT models. The same is true also for the fifth mode that describes unidentical longitudinal movements of the face sheets. The last two modes of the HSAPT and EHSAPT are quite different than those of the elasticity solution although there is a good correlation of the corresponding eigenfrequencies.

The modes through the depth of the panel appear in Figure 7 for the first seven modes that correspond to the first half wave number. Here the normalization is with respect to the extreme value of the longitudinal or the vertical displacements in all models. In the first mode the distribution of the longitudinal displacement is in the form of a zig-zag curve and the vertical displacements changes within the depth of the core and all model correlate well. The same is true also for the second mode. Here, the vertical displacement in the core is linear and the longitudinal is parabolic. In all the higher modes the HSAPT and EHSAPT results compare very well with the elasticity solution.

Multi-layered core

The second case uses the experimental setup that appears in Gardner et al. [26] (configuration 2 in Figure 3). Geometry and mechanical properties are provided in Figure 8. Here, the layout of the sandwich panel is non-symmetric through its depth. The response of this case has been determined using the elasticity model with a number of layers within the core. The results are compared with the case of a uniform core of equivalent properties (Table 2). They reveal that the models that use the

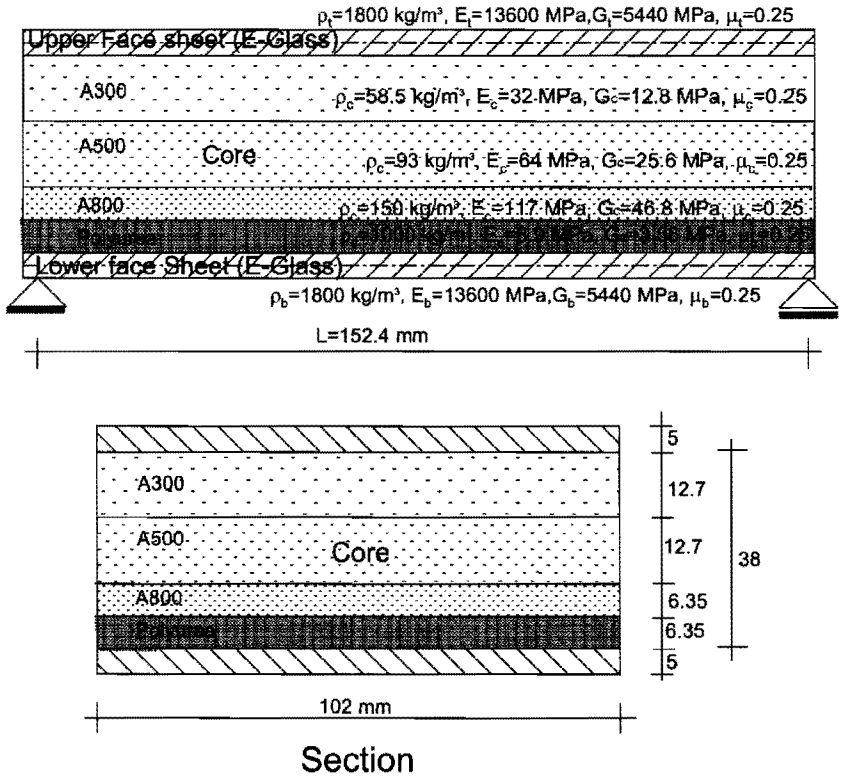

Figure 8. Layout of a sandwich panel with a multi-layered core and a typical section.

Table 2. Eigenfrequencies of a multi-layered core (see Figure11), with an equivalent and a multi-layered core using the elasticity models.

Mode no.	1	2	3	4	5	6	7
Equivalent core	0.175	0.680	1.092	1.824	2.063	2.321	2.575
Multi-layered core	0.137	0.513	0.803	1.308	1.562	2.209	2.378

equivalent properties yield higher values than those of the elasticity solution probably because of the different distribution of the masses through the depth of the core.

The distribution of the displacements and the stresses through the depth of the panel for the modes that correspond to the first half-wave number appear in Figure 9. In the first mode the displacements in the face sheets are quite similar for both cases but in the core the discrepancies are larger for the in-plane displacement and insignificant for the vertical one. The in-plane normal stresses, σ_{xx}, in the face sheet and the core are very similar although with different values. Here, the normal in-plane stresses are practically null although the in-plane rigidity of

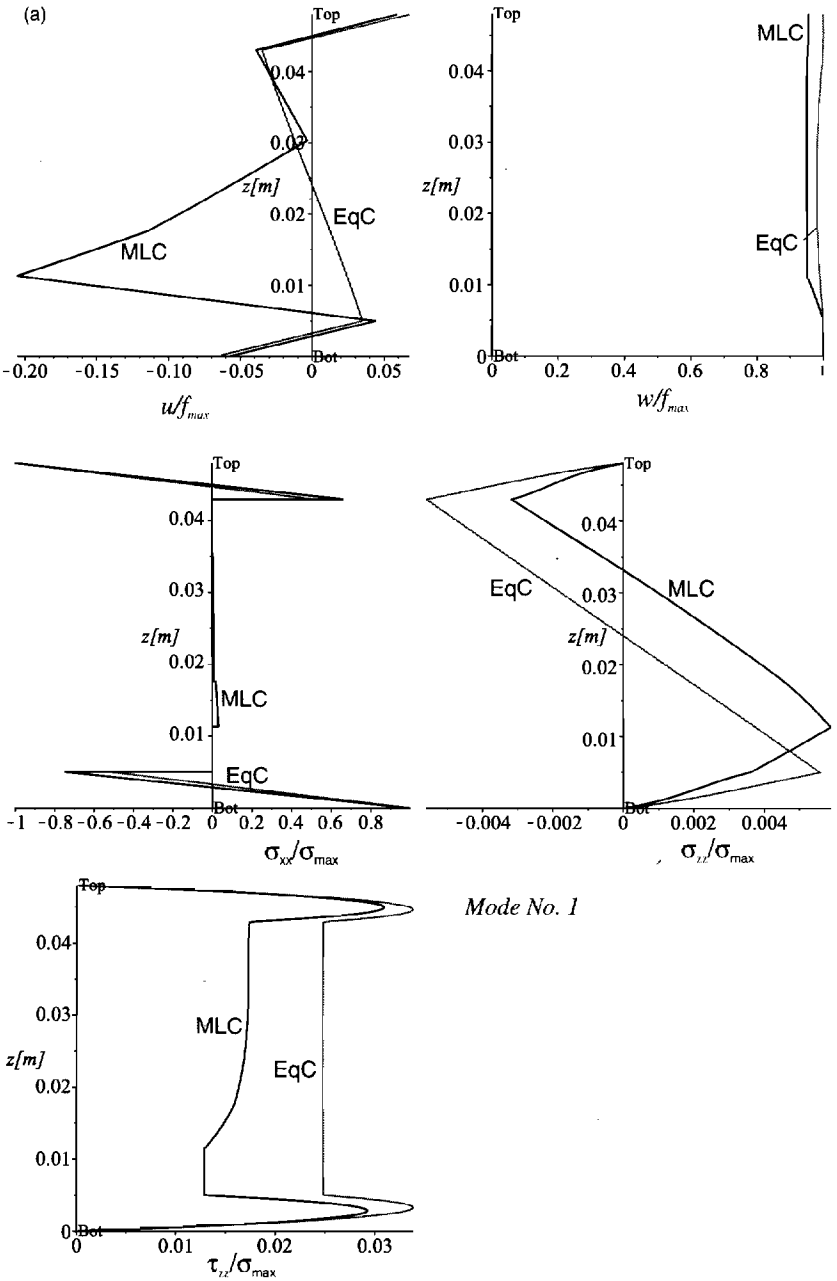

Figure 9. Two eigenmodes of displacements and stresses of the first half-wave number through depth of panel for the equivalent and multi-layered configuration: (a) first eigenmodes and (b) second eigenmodes.

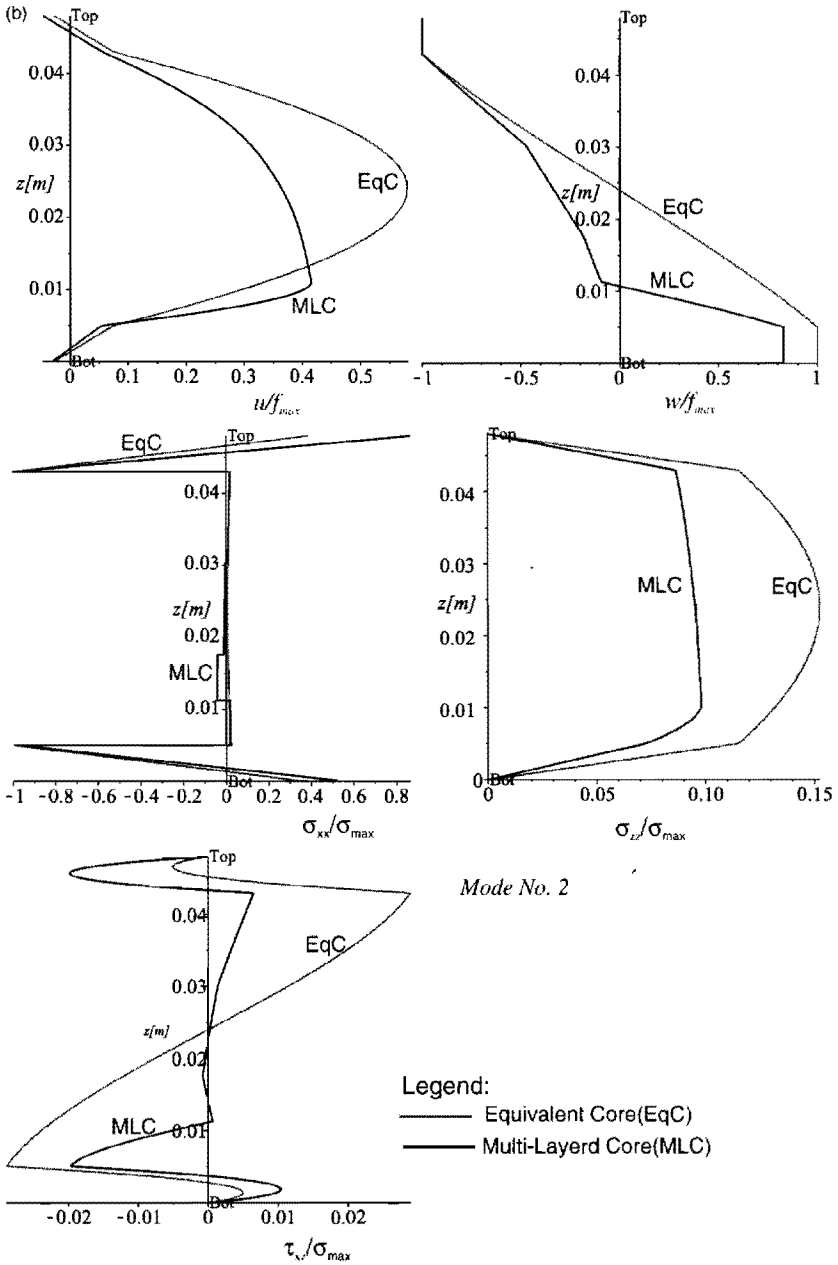

Figure 9. Continued.

the core is considered. The discrepancy in the vertical normal stresses, σ_{zz}, and the shear stresses, τ_{xz}, is in their values while the patterns are very similar. In the pumping mode, the second eigenmode, the differences between the two models are in the displacement patterns of the core while the displacements in the face sheets are almost identical. The in-plane normal stresses in the core are very similar and again with very small values. In the vertical normal and shear stresses the differences are much more pronounced in the core, but with similar patterns in the face sheets.

Summary and conclusions

The investigations include a brief rigorous systematic analysis of the problem of free vibrations of sandwich panels with compressible compliant core using high-order models and an elasticity model with isotropic and orthotropic mechanical properties and a numerical study. The model formulations are based on Hamilton's principle with appropriate kinematic relations of small deformations. It includes high-order models of the HSAPT with mixed formulation that includes displacements of the face sheets and shear stress in core as unknowns, the HSAPT with displacements as unknowns and assuming cubic and quadratic distributions of the displacements within the core but with negligible in-plane rigidity and the EHSAPT that uses the cubic and quadratic distribution for the displacement patterns within the core but it includes the in-plane rigidity of the core in the analysis. The benchmark solution is the closed-form solution of the elasticity model for the case of isotropic or orthotropic simply-supported sandwich panel. Notice that the general equations of motion for all computational models are valid for any type of layout of the sandwich panel and to any boundary conditions. In all models the mass and the stiffness matrices have been derived for the particular case of a simply-supported panel of any construction of the sandwich panel.

The numerical study uses a particular sandwich panel setup that has been used for blast response in the University of Rhode Island [26]. Two types of panels have been considered with a single- and a multi-layered core. In the first case the study looked into the response of a light and a heavy core, eigenfrequencies and modes of first and second half-wave numbers and comparison with elasticity and FE models. The results reveal that the first mode can be detected accurately by all models while the higher ones can be detected correctly only by the HSAPT (displacement) and the EHSAPT models. The introduction of the heavy core with larger moduli of elasticity and shear and specific weight follows the same trends. The comparison of the FE results with the elasticity ones reveals good correlation. The correlations with eigenmodes longitudinally and through the depth of the panel are similar in the first mode for all models. They are quite different from the elasticity solution for the higher modes except for the EHSAPT and HSAPT models that use the displacement formulation.

In the second case with the multi-layered core the study compares the response of a sandwich panel with an equivalent single material core with that with a multi-

layered core using the elasticity solution. Notice that the multi-layered construction of the core is un-symmetric and includes a very heavy layer, polyurea, at the bottom of the core but with a very small elasticity and shear moduli. Hence, the mass distribution through the depth of the panel with the multi-layered core is quite different than that of the equivalent one. The results include the eigenfrequencies and displacements and stress distribution through depth of panel. The eigenfrequencies of the equivalent panel are larger than those of multi-layered construction while the modes of the displacements and stresses in the face sheets are similar and significant differences in the core. The differences are attributed to the differences in the distribution of the mass through the depth of the core between the two schemes.

The comparison between the various computational models and the elasticity solution reveals that the EHSAPT and the HSAPT with the displacement formulation yield accurate results in terms of eigenfrequencies and eigenmodes. Hence, in the case of a sandwich panel with a general construction layout and general boundary conditions the layered HSAPT or EHSAPT formulation should be used with accuracy.

Acknowledgment

The finite elements runs of ADINA have been conducted by Prof. I Sheinman of Technion. His assistance is gratefully acknowledged.

Conflict of interest

None declared.

Funding

The research has been supported by the Office of Naval Research [Grant N00014-11-1-0597] and the Ashtrom Engineering Company that supports the professorship chair of Prof. Frostig. The ONR program manager was Dr Yapa DS Rajapakse. His interest, encouragements and the financial support received are gratefully acknowledged.

References

1. Allen HG. *Analysis and design of structural sandwich panels.* London: Pergamon Press, 1969.
2. Plantema FJ. *Sandwich construction.* New York: John Wiley and Sons, 1966.
3. Vinson JR. *The behavior of sandwich structures of isotropic and composite materials.* Lancaster: Technomic Publishing Co. Inc, 1999.
4. Frostig Y, Baruch M, Vilnay O, et al. A high order theory for the bending of sandwich beams with a flexible core. *J ASCE, EM Div* 1992; 118(5): 1026–1043.
5. Pagano NJ. Exact solutions for rectangular bidirectional composites and sandwich plates. *J Compos Mater* 1970; 4: 20–34.
6. Pagano NJ and Hatfield SJ. Elastic behavior of multilayered bidirectional composites. *AIAA J* 1972; 10(7): 931–933.
7. Zenkour AM. Three-dimensional elasticity solution for uniformly loaded cross-ply laminates and sandwich plates. *J Sandwich Struct Mater* 2007; 9: 213–238.

8. Kardomateas GA. Three dimensional elasticity solution for sandwich plates with orthotropic phases: the positive discriminant case. *J Appl Mech (ASME)* 2009; 76: 014505-1–014505-4.
9. Kardomateas GA. An elasticity solution for the global buckling of sandwich beams/wide panels with orthotropic phases. *J Appl Mech (ASME)* 2010; 77(2): 021015-1–021015-7.
10. Kardomateas GA and Phan CN. Three-dimensional elasticity solution for sandwich beams/wide plates with orthotropic phases: the negative discriminant case. *J Sandwich Struct Mater* 2011; 13(6): 641–661.
11. Srinivas S and Rao AK. Bending, vibration and buckling of simply supported thick orthotropic rectangular plates and laminates. *Int J Solids Struct* 1970; 6: 1463–1481.
12. Karczmarzyk S. A new 2d single series model of transverse vibration of a multilayered sandwich beam with perfectly clamped edges. *J Theor Appl Mech* 2010; 48(3): 789–812.
13. Frostig Y and Baruch M. Buckling of simply-supported sandwich beams with transversely flexible core - a high order theory. *J ASCE, EM Div* 1993; 119(3): 476-495.
14. Frostig Y and Baruch M. Free vibration of sandwich beams with a transversely flexible core: a high order approach. *J Sound Vib* 1994; 176(2): 195–208.
15. Sokolinsky V and Frostig Y. Branching behavior in the non-linear response of sandwich panels with a transversely flexible core. *Int J Solids Struct* 2000; 37: 5745–5772.
16. Bozhevolnaya E and Frostig Y. Free vibration of curved sandwich beams with a transversely flexible core. *J Sandwich Struct Mater* 2001; 3(4): 311–342.
17. Frostig Y and Thomsen OT. High-order free vibration of sandwich panels with a flexible core. *Int J Solids Struct* 2004; 41(5-6): 1697–1724.
18. Schwarts-Givli H, Rabinovitch O and Frostig Y. High order nonlinear contact effects in the dynamic behavior of delaminated sandwich panels with flexible core. *Int J Solids Struct* 2007; 44(1): 77–99.
19. Schwarts-Givli H, Rabinovitch O and Frostig Y. High-order free vibrations of delaminated simply supported sandwich panels with a transversely flexible core – a modified Galerkin approach. *J Sound Vib* 2007; 301(1–2): 253–277.
20. Frostig Y and Thomsen. On the free vibration of sandwich panels with a flexible and material temperature dependent core - Part I – Mathematical formulation. *Compos Sci Technol* 2009; 69(6): 856–862.
21. Frostig Y and Thomsen OT. On the vibration of sandwich panels with a flexible and material temperature dependent core - Part II – Numerical study. *Compos Sci Technol* 2009; 69(6): 863–869.
22. Frostig Y. On wrinkling of a sandwich panel with a compliant core and self-equilibrated loads. *J Sandwich Struct Mater* 2011; 13(6): 663–679.
23. Phan CN, Bailey NW, Kardomateas GA, et al. Wrinkling of sandwich wide panels/beams based on the extended high order sandwich panel theory: formulation, comparison with elasticity and experiments. *Arch Appl Mech* 2012; 82(10–11): 1585–1599.
24. Phan CN, Kardomateas GA and Frostig Y. Global buckling of a sandwich wide panel/beam based on the extended high order theory. *AIAA J*, Paper No: 2011-06-J051454 (In press).
25. Phan CN. *The extended high-order sandwich panel theory*, PhD Thesis, Georgia Institute of Technology, USA, 2011.

26. Gardner N, Wang E, Kumar P, et al. Blast mitigation in a sandwich composite using graded core and polyurea interlayer. *Exp Mech* 2012; 52(2): 119–133.

Appendix I

HSAPT (displacement formulation) – Equations of motion

$$\left(\left(\frac{1}{30}-\frac{7}{30}\frac{d_b}{c}\right)w_{b,x}+\left(-\frac{19}{30}-\frac{47}{30}\frac{d_t}{c}\right)w_{t,x}\right.$$
$$\left.-\frac{7}{15}\frac{u_{ob}}{c}+\frac{47}{15}\frac{u_{ot}}{c}+\frac{4}{5}\phi-\frac{2}{5}\frac{\mathrm{d}}{\mathrm{d}x}w_o(x)-\frac{8}{3}\frac{u_{oc}}{c}\right)b_wG_{xzc}$$
$$+\left(-\frac{1}{70}c\phi_{tt}-\frac{3}{70}w_{t,xtt}d_t+\frac{3}{35}u_{ot,tt}+\frac{1}{140}w_{b,xtt}d_b+\frac{1}{15}u_{oc,tt}+\frac{1}{70}u_{ob,tt}\right)M_c$$
$$+M_tu_{ot,tt}-EA_tu_{ot,xx}=0 \tag{24}$$

$$\left(-\frac{8}{3}\frac{w_o(x)}{c}+\frac{7}{3}\frac{w_t}{c}+\frac{1}{3}\frac{w_b}{c}+\frac{1}{3}\frac{w_b}{c}\right)b_wE_{zc}+\left(\left(\frac{1}{60}d_b+\frac{1}{60}d_t+\frac{1}{30}c-\frac{7}{60}\frac{d_td_b}{c}\right)w_{b,xx}\right.$$
$$+\left(-\frac{2}{15}c-\frac{19}{30}d_t-\frac{47}{60}\frac{d_t^2}{c}\right)w_{t,xx}+\left(\frac{1}{30}-\frac{7}{30}\frac{d_t}{c}\right)u_{ob,x}+\left(\frac{19}{30}+\frac{47}{30}\frac{d_t}{c}\right)u_{ot,x}$$
$$\left.-\frac{1}{5}\left(\frac{\mathrm{d}_2}{\mathrm{d}x^2}w_o(x)\right)d_t-\frac{4}{3}\frac{u_{oc,x}d_t}{c}+\frac{2}{5}\phi d_t-\frac{1}{15}\left(\frac{\mathrm{d}^2}{\mathrm{d}x^2}w_o(x)\right)c-\frac{2}{3}u_{oc,x}+\frac{2}{15}\phi_xc\right)b_cG_c$$
$$+\frac{3}{70}u_{ot,xtt}d_t+\frac{1}{30}d_tu_{oc,xtt}-\frac{1}{30}w_{b,tt}-\frac{3}{140}w_{t,xxtt}d_t^2+\frac{1}{280}w_{b,xxtt}d_bd_t+\frac{2}{15}w_{t,tt}$$
$$\left.+\frac{1}{140}u_{o,bxtt}d_t-\frac{1}{140}cd_t\phi_{xtt}\right)M_c-w_{t,xxtt}\mathrm{I}_{mt}+EI_tw_{t,xxxx}+M_tw_{t,tt}=0 \tag{25}$$

$$\left(\left(\frac{47}{30}\frac{d_b}{c}+\frac{19}{30}\right)w_{b,x}+\left(-\frac{1}{30}+\frac{7}{30}\frac{d_t}{c}\right)w_{t,x}-\frac{4}{5}\phi\right.$$
$$\left.-\frac{8}{3}\frac{u_{oc}}{c}+\frac{2}{5}\frac{\mathrm{d}}{\mathrm{dx}}w_o(x)+\frac{47}{15}\frac{u_{ob}}{c}-\frac{7}{15}\frac{u_{ot}}{c}\right)b_wG_{zc}$$
$$+\left(\frac{1}{15}u_{oc,tt}+\frac{3}{35}u_{ob,tt}-\frac{1}{140}w_{t,xtt}d_t+\frac{3}{70}w_{b,xtt}d_b+\frac{1}{70}c\phi_{tt}+\frac{1}{70}u_{ot,tt}\right)M_c$$
$$+M_bu_{ob,tt}-EA_bu_{ob,xx}=0 \tag{26}$$

$$\left(-\frac{8}{3}\frac{w_0(x)}{c}+\frac{7}{3}\frac{w_b}{c}+\frac{1}{3}\frac{w_t}{c}\right)b_wE_{zc}+\left(\left(-\frac{47}{60}\frac{d_b^2}{c}-\frac{2}{15}c-\frac{19}{30}d_b\right)w_{b,xx}\right)$$
$$+\left(\frac{1}{60}d_b+\frac{1}{60}d_t+\frac{1}{30}c-\frac{7}{60}\frac{d_td_b}{c}\right)w_{t,xx}+\left(-\frac{47}{30}\frac{d_b}{c}-\frac{19}{30}\right)u_{ob,x}$$
$$+\left(\frac{7}{30}\frac{d_b}{c}-\frac{1}{30}\right)u_{ot,x}-\frac{1}{15}\left(\frac{\mathrm{d}^2}{\mathrm{d}x^2}w_o(x)\right)c+\frac{2}{3}u_{oc,x}+\frac{2}{15}\phi_xc$$
$$-\frac{1}{5}\left(\frac{\mathrm{d}^2}{\mathrm{d}x^2}w_o(x)\right)d_b+\frac{4}{3}\frac{u_{oc,x}d_b}{c}+\frac{2}{5}\phi_xd_b\Bigg)b_cG_c+\left(\frac{1}{280}w_{t,xxtt}d_td_b\right.$$
$$-\frac{1}{140}u_{ot,xtt}d_b-\frac{1}{140}cd_b\phi_{xtt}-\frac{3}{140}w_{b,xxtt}d_b^2-\frac{1}{30}w_{t,tt}+\frac{2}{15}w_{b,tt}$$
$$\left.-\frac{1}{30}d_bu_{oc,xtt}-\frac{3}{70}u_{o,bxtt}d_b\right)M_c-w_{b,xxtt}\mathbf{I}_{mb}+EI_bw_{b,xxxx}+M_bw_{b,tt}=0 \tag{27}$$

$$\left(\left(-\frac{2}{3}-\frac{4}{3}\frac{d_b}{c}\right)w_{b,x}+\left(\frac{4}{3}\frac{d_t}{c}+\frac{2}{3}\right)w_{t,x}+\frac{16}{3}\frac{u_{oc}}{c}-\frac{8}{3}\frac{u_{ob}}{c}-\frac{8}{3}\frac{u_{ot}}{c}\right)b_wG_{zc}$$
$$+\left(\frac{8}{15}u_{oc,tt}+\frac{1}{15}u_{ob,tt}+\frac{1}{15}u_{ot,tt}+\frac{1}{30}w_{b,xtt}d_b-\frac{1}{30}w_{t,xtt}d_t\right)M_c=0 \tag{28}$$

$$\left(\left(-\frac{2}{15}c-\frac{2}{5}d_b\right)w_{b,x}+\left(-\frac{2}{5}d_t-\frac{2}{15}c\right)w_{t,x}+\frac{4}{5}\phi c+\frac{4}{15}\left(\frac{\mathrm{d}}{\mathrm{d}x}w_o(x)\right)c-\frac{4}{5}u_{ob}+\frac{4}{5}u_{ot}\right)$$
$$\times b_wG_{zc}+\left(\frac{1}{70}cu_{ob,tt}+\frac{2}{105}c^2\phi_{tt}+\frac{1}{140}cd_bw_b,xtt-\frac{1}{170}cu_{ot,tt}+\frac{1}{140}cd_tw_{t,xtt}\right)M_c=0 \tag{29}$$

$$\left(\frac{16}{3}\frac{w_o(x)}{c}-\frac{8}{3}\frac{w_b}{c}-\frac{8}{3}\frac{w_t}{c}\right)b_wE_{zc}+\left(\left(-\frac{1}{5}d_b-\frac{1}{15}c\right)w_{b,xx}+\left(-\frac{1}{15}d_t-\frac{1}{15}c\right)w_{t,xx}\right.$$
$$-\frac{2}{5}u_{ob,x}+\frac{2}{5}u_{ot,x}--\frac{4}{15}\phi_xc-\frac{8}{15}\left(\frac{\mathrm{d}^2}{\mathrm{d}x^2}w_o(x)\right)c\Bigg)b_cG_c$$
$$+\left(\frac{1}{15}w_{b,tt}+\frac{1}{15}w_{t,tt}\right)M_c=0 \tag{30}$$

Appendix 2

EHSAPT – Equations of motion

$$\left(\left(\frac{1}{30}-\frac{7}{30}\frac{d_b}{c}\right)w_{b,x}+\left(-\frac{19}{30}-\frac{47}{30}\frac{d_t}{c}\right)w_{t,x}-\frac{7}{15}\frac{u_{ob}}{c}+\frac{47}{15}\frac{u_{ot}}{c}+\frac{4}{5}\phi\right.$$

$$-\frac{2}{5}\frac{\mathrm{d}}{\mathrm{d}x}w_o(x)-\frac{8}{3}\frac{u_{oc}}{c}\Big)b_wG_{xzc}+\Big(-\frac{1}{70}c\phi_{tt}-\frac{3}{70}w_{t,xtt}d_t+\frac{3}{55}u_{ot,tt}$$
$$+\frac{1}{140}w_{b,xtt}d_b+\frac{1}{15}u_{oc,tt}+\frac{1}{70}u_{ob,tt}\Big)M_c+M_tu_{ot,tt}-EA_tu_{ot,xx}=0 \qquad (31)$$

$$\Big(\Big(\frac{1}{60}d_b+\frac{1}{60}d_t+\frac{1}{30}c-\frac{7}{60}\frac{d_td_b}{c}\Big)w_{b,xx}+\Big(-\frac{1}{5}d_t-\frac{1}{15}c\Big)\Big(\frac{\partial^2}{\partial x^2}w_o(x,t)\Big)$$
$$+\Big(-\frac{2}{15}c-\frac{19}{30}d_t-\frac{47}{60}\frac{d_t^2}{c}\Big)w_{t,xx}+\Big(\frac{2}{15}c+\frac{2}{5}d_t\Big)\phi_x+\Big(\frac{1}{30}-\frac{7}{30}\frac{d_t}{c}\Big)u_{ob,x}$$
$$+\Big(-\frac{4}{3}\frac{d_t}{c}-\frac{2}{3}\Big)u_{oc,x}+\Big(\frac{19}{30}+\frac{47}{30}\frac{d_t}{c}\Big)u_{ot,x}\Big)b_wG_c$$
$$+\Big(-\frac{1}{30}w_{b,tt}+\frac{2}{15}w_{t,tt}\Big)M_c+EI_tw_{t,xxxx}+M_tw_{t,tt}-w_{t,xxtt}\mathrm{I}_{mt}$$
$$+\frac{1}{-\mu_c^2+1}\Big(\Big(\Big(\Big(\Big(\frac{1}{60}d_t+\frac{1}{60}d_b\Big)w_{b,xx}-\frac{11}{30}u_{ot,x}-\frac{1}{5}\Big(\frac{\partial^2}{\partial x^2}w_o(x,t)\Big)d_t$$
$$-\frac{2}{3}u_{oc,x}+\frac{11}{30}w_{t,xx}d_t+\frac{2}{15}\phi_xc+\frac{1}{30}u_{ob,x}\Big)\mu_c-\frac{3}{70}cd_tu_{ot,xxx}$$
$$+\frac{3}{140}w_{t,xxxx}cd_t^2+\frac{1}{3}\frac{w_b}{c}-\frac{1}{140}cd_tu_{ob,xxx}-\frac{1}{280}cd_bd_tw_{b,xxxx}$$
$$+\frac{1}{140}c^2d_t\phi_{xxx}-\frac{1}{30}cd_tu_{oc,xxx}+\frac{7}{3}\frac{w_t}{c}-\frac{8}{3}\frac{w_o(x)}{c}\Big)b_wE_c\Big)=0 \qquad (32)$$

$$\Big(\Big(\frac{47}{30}\frac{d_b}{c}+\frac{19}{30}\Big)w_{b,x}+\frac{2}{5}\frac{\partial}{\partial x}w_o(x,t)+\Big(-\frac{1}{30}+\frac{7}{30}\frac{d_t}{c}\Big)w_{t,x}-\frac{7}{15}\frac{u_{ot}}{c}$$
$$+\frac{47}{15}\frac{u_{ob}}{c}-\frac{8}{3}\frac{u_{oc}}{c}-\frac{4}{5}\phi\Big)b_wG_c+\Big(\frac{1}{15}u_{oc,tt}+\frac{3}{35}u_{ob,tt}-\frac{1}{140}w_{t,xtt}d_t$$
$$+\frac{3}{70}w_{b,xtt}d_b+\frac{1}{70}c\phi_{tt}+\frac{1}{70}u_{oc,tt}\Big)M_c+M_bu_{ob,tt}-EA_bu_{ob,xx}$$
$$+\frac{1}{-\mu_c^2+1}\Big(\Big(\Big(\Big(-\frac{1}{30}w_{t,x}+\frac{2}{5}\frac{\partial}{\partial x}w_o(x,t)-\frac{11}{30}w_{b,x}\Big)\mu_c$$
$$-\frac{3}{70}cd_bw_{b,xxx}-\frac{1}{70}u_{ot,xx}c-\frac{1}{15}cu_{oc,xx}-\frac{1}{70}c^2\phi_{xx}-\frac{3}{35}cu_{ob,xx}\Big)$$
$$+\frac{1}{140}c_{wt,xxx}d_t\Big)b_wE_c\Big)=0 \qquad (33)$$

$$\left(\left(-\frac{47}{60}\frac{d_b^2}{c}-\frac{2}{15}c-\frac{19}{30}d_b\right)w_{b,xx}+\left(-\frac{1}{5}d_b-\frac{1}{15}c\right)\left(\frac{\partial^2}{\partial x_2}w_o(x,t)\right)\right.$$
$$+\left(\frac{1}{60}d_b+\frac{1}{60}d_t+\frac{1}{30}c-\frac{7}{60}\frac{d_td_b}{c}\right)w_{t,xx}+\left(\frac{2}{5}d_b+\frac{2}{15}c\right)\phi_x$$
$$+\left(-\frac{47}{30}\frac{d_b}{c}-\frac{19}{30}\right)u_{ob,x}+\left(\frac{4}{3}\frac{d_b}{c}+\frac{2}{3}\right)u_{oc,x}+\left(\frac{7}{30}\frac{d_b}{c}-\frac{1}{30}\right)u_{ot,x}\Big)b_wG_c$$
$$+\left(\frac{2}{15}w_{b,tt}-\frac{1}{30}w_{t,tt}\right)M_c+EI_bw_{b,xxxx}+M_bw_{b,tt}-w_{b,xxtt}\mathrm{I}_{mb}$$
$$+\frac{1}{-\mu_c^2+1}\left(\left(\left(\frac{11}{30}w_{b,xx}d_b-\frac{1}{5}\left(\frac{\partial^2}{\partial x^2}w_o(x,t)\right)d_b+\left(\frac{1}{60}d_t+\frac{1}{60}d_b\right)w_{t,xx}+\frac{2}{15}\phi_xc\right.\right.\right.$$
$$\left.+\frac{2}{3}u_{oc,x}+\frac{1}{30}u_{ot,x}+\frac{11}{30}u_{ob,x}\right)\mu_c-\frac{1}{280}w_{t,xxxx}cd_td_b+\frac{7}{3}\frac{w_b}{c}-\frac{8}{3}\frac{w_o(x)}{c}+\frac{1}{3}\frac{w_t}{c}$$
$$+\frac{1}{140}cd_bu_{ot,xxx}+\frac{1}{140}c^2d_b\phi_{xxx}+\frac{1}{30}cd_bu_{oc,xxx}$$
$$\left.+\frac{3}{70}cd_bu_{ob,xxx}+\frac{3}{140}w_{b,xxxx}cd_b^2\right)b_wE_c\Big)=0 \tag{34}$$

$$\left(\left(-\frac{2}{3}-\frac{4}{3}\frac{d_b}{c}\right)w_{b,x}+\left(\frac{4}{3}\frac{d_t}{c}+\frac{2}{3}\right)w_{t,x}+\frac{16}{3}\frac{u_{oc}}{c}-\frac{8}{3}\frac{u_{ob}}{c}-\frac{8}{3}\frac{u_{ot}}{e}\right)b_wG_c$$
$$+\left(\frac{8}{15}u_{oc,tt}+\frac{1}{15}u_{ob,tt}+\frac{1}{15}u_{ot,tt}+\frac{1}{30}w_{b,xtt}d_b-\frac{1}{30}w_{t,xtt}d_t\right)M_c$$
$$+\frac{1}{-\mu_c^2+1}\left(\left(\left(-\frac{2}{3}w_{b,x}+\frac{2}{3}w_{t,x}\right)\mu_c-\frac{8}{15}cu_{oc,xx}-\frac{1}{15}u_{ot,xx}c+\frac{1}{30}cw_{t,xxx}d_t\right.\right.$$
$$\left.-\frac{1}{15}cu_{ob,xx}-\frac{1}{30}cd_bw_{b,xxx}\right)b_wE_c\Big)=0 \tag{35}$$

$$\left(\left(-\frac{2}{15}c-\frac{2}{15}d_b\right)w_{b,x}+\frac{4}{15}\left(\frac{\partial}{\partial x}w_o(x,t)\right)c+\left(-\frac{2}{5}d_t-\frac{2}{15}c\right)w_{t,x}+\frac{4}{5}u_{ot}\right.$$
$$-\frac{4}{5}u_{ob}+\frac{4}{5}\phi c\Big)b_wG_c+\left(\frac{1}{70}cu_{ob,tt}+\frac{2}{105}c^2\phi_{tt}+\frac{1}{140}cd_bw_{b,xtt}\right.$$
$$-\frac{1}{70}cu_{ot,tt}+\frac{1}{140}cd_tw_t,xtt\Big)M_c+\frac{1}{-\mu_c^2+1}\left(\left(\left(\frac{4}{15}\left(\frac{\partial}{\partial x}w_o(x,t)\right)c\right.\right.\right.$$
$$-\frac{2}{15}w_{b,x}c-\frac{2}{15}w_{t,x}c\Big)\mu_c-\frac{1}{70}c^2u_{ob,xx}-\frac{1}{140}c^2d_bw_{b,xxx}$$
$$\left.-\frac{1}{140}c^2w_{t,xxx}d_t-\frac{2}{105}c^3\phi_{xx}+\frac{1}{70}c^2u_{ot,xx}\right)b_wE_c\Big)=0 \tag{36}$$

$$\left(\left(-\frac{2}{15}c-\frac{2}{5}d_b\right)w_{b,x}+\frac{4}{15}\left(\frac{\partial}{\partial x}w_o(x,t)\right)c+\left(-\frac{2}{5}d_t-\frac{2}{15}c\right)w_{t,x}+\frac{4}{5}u_{ot}\right.$$
$$-\frac{4}{5}u_{ob}+\frac{4}{5}\phi c\Big)b_wG_c+\left(\frac{1}{70}cu_{ob,tt}+\frac{2}{105}c^2\phi_{tt}+\frac{1}{140}cd_bw_{b,xtt}\right.$$
$$-\frac{1}{70}cu_{ot,tt}+\frac{1}{140}cd_tw_{t,xtt}\Big)M_c+\frac{1}{-\mu_c^2+1}\left(\left(\left(\frac{4}{15}\left(\frac{\partial}{\partial x}w_o(x,t)\right)c\right.\right.\right.$$
$$-\frac{2}{15}w_{b,x}c-\frac{2}{15}w_{t,x}c\Big)\mu_c-\frac{1}{70}c^2u_{ob,xx}-\frac{1}{140}c^2d_bw_{b,xxx}$$
$$\left.-\frac{1}{140}c^2w_{t,xxx}d_t-\frac{2}{105}c^3\phi_{xx}+\frac{1}{70}c^2u_{ot,xx}\right)b_wE_c\Big)=0 \tag{37}$$